European Commission
Research Programme of the Research Fund for Coal and Steel

ANGELHY

Innovative solutions for design and strengthening of telecommunications and transmission lattice towers using large angles from high strength steel and hybrid techniques of angles with FRP strips

WORK PACKAGE 4 – DELIVERABLE 4.2

SAFETY ESTIMATES AND COST-BENEFIT ANALYSES OF CASE STUDIES

Coordinator:

National Technical University of Athens - NTUA, Greece

Beneficiaries:

ArcelorMittal Belval & Differdange SA - AMBD, Luxembourg

Universite de Liege - ULG, Belgium

COSMOTE Kinites Tilepikoinonies AE - COSMOTE, Greece

Centre Technique Industriel de la Construction Metallique - CTICM, France

SIKA France SAS - SIKA, France

Grant Agreement Number: 753993

31/12/2020

AUTHORS:

NATIONAL TECHNICAL UNIVERSITY OF ATHENS

Institute of Steel Structures

Iroon Polytechniou 9, 15780 Athens, Greece

Authors: Dimitrios V. Bilionis, Angeliki Gerontati, Dimitrios Vamvatsikos

TABLE OF CONTENTS

1 Introduction

Task 4.2 of the ANGELHY project was associated with the performance-based assessment of steel lattice towers. A performance-based assessment mainly aims to the estimation of the risk of a specific structure and its associated costs. The risk of a specific structure depends on two legs: first the fragility of the structure which is actually related to its strength and secondly the hazard of its location.

Herein, the risk of all the models of the steel lattice towers considered in Task 4.1 and summarized in Table 1.1 was assessed. The fragility of each model was estimated based on the results of numerous non-linear dynamic analyses for various scenarios of loads. For the estimation of hazard, meteorological data from two different countries were elaborated. In specific for the case of the telecommunicaton towers the site of installation was assumed to be coastal areas of Greece. On the other hand for the power transmisssion towers the location was assumed to be a site in Central-East Germany. It is evident that both locations are expected to have very different meteorological characteristics due to their different climate.

Finally, based on the results of the risk estimation, a connection with economic aspects was attempted by performing cost-benefit analyses considering current market values.

Table 1.1: Types of Lattice Towers Considered

Telecommunication Tower	**Suspension Transmission Tower**	**Dead-End Transmission Tower**
Initial State	Initial State	Initial State
Corroded State	Corroded State	Corroded State
Strengthened Hybrid	-	Strengthened Hybrid
High Strength Steel (HSS) tower	High Strength Steel (HSS) tower	High Strength Steel (HSS) tower
Location: Greece	**Location:** Germany	**Location:** Germany

2 Risk Assessment Methodology

2.1 Fragility Estimation

Fragility could be defined as the probability of failure for a given intensity measure (IM), herein the value of wind speed. The results of such an analysis are reported in the form of fragility curves. The estimation of the fragility functions and corresponding curves is based on the probability of failure for the various values of the IM, i.e. the wind speed in this case. A common assumption is that the fragility curve is defined by a lognormal cumulative function (CDF) with the following mathematical expression [1]:

$$P(C|IM = x) = \Phi\left(\frac{ln(x/\theta)}{\beta}\right) \quad \text{Eq. 2.1}$$

where:

$P(C|IM = x)$ is the probability that a value of the IM (e.g. the wind speed) equal to x will cause a failure of the structure, $\Phi(\cdot)$ is the standard normal cumulative distribution function (CDF), θ is the median of the fragility function which corresponds to the value of IM with 50% probability of failure and β is the standard deviation of *lnIM*, sometimes referred to as dispersion of IM.

A simple method to estimate fragility is by performing stripe analysis. Stripe analysis is mainly applied when discrete values of IM are used. The first step of the process is to perform a number of dynamic analyses for each value of the IM, herein the wind speed, and then estimate the number of cases where a failure has occurred. Then for each wind speed the fraction of analyses causing failure could be estimated by simply dividing their number by the total number of analyses. This fraction is actually an estimator of the probability of failure for the corresponding value of the IM.

The next step is to fit a lognormal cumulative function (Eq. (2.1)) to the values of the probability of failure for each of the IM values. The parameters θ and β can be easily estimated by maximum likelihood estimation method as in [1]. Furthermore, the dispersion can be modified in order to account for the uncertainties in steel angle buckling resistance by considering values of dispersion that have been observed in relevant laboratory tests. Thus, the total dispersion is estimated as:

$$\beta_{total} = \sqrt{{\beta_R}^2 + {\beta_u}^2} \quad \text{Eq. 2.2}$$

where:

β_R is the dispersion estimated from the analyses (i.e. the lognormal fitting) and β_u the dispersion attributed to member tests as proposed by [2].

2.2 Hazard Assessment

2.2.1 Wind Hazard

For the estimation of the wind hazard, meteorological data from the closest weather station should be obtained. In specific, detailed time-histories of wind speed and direction are usually available in 10min resolution. Processing the above data could provide the probability distribution of wind speed and direction (i.e. wind rose) which corresponds to the wind hazard of a location. Typical forms of the distribution of wind speed and direction are shown in Figure 2.1.

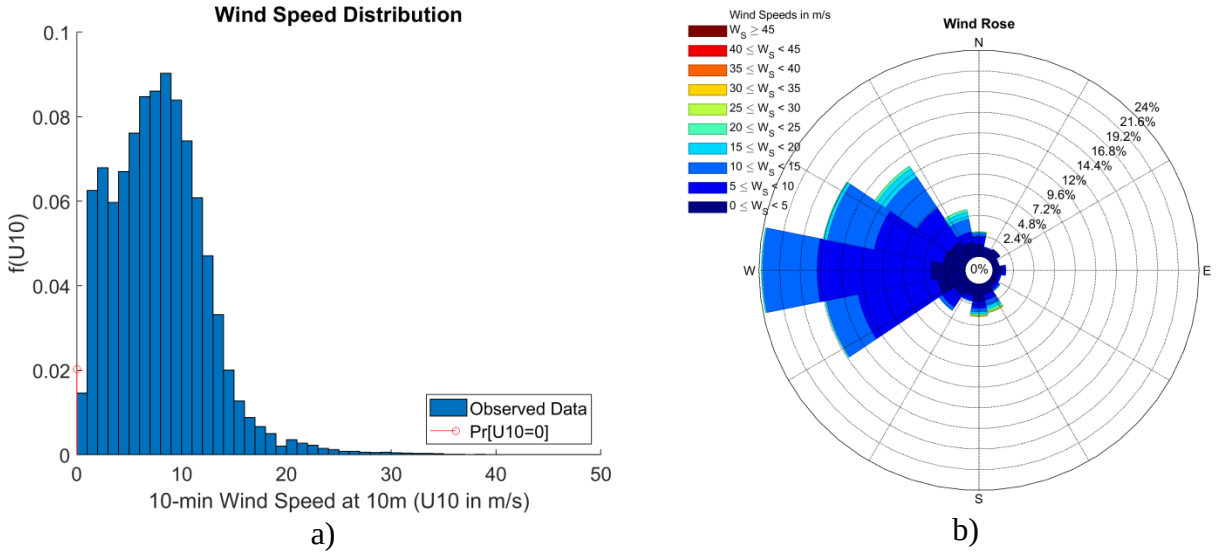

a) b)

Figure 2.1: Typical Forms of Distribution of: a) Wind Speed and b) Wind Direction (Wind Rose)

2.2.2 Icing Hazard

In practice there is no directly measured information about the ice thickness from meteorological stations. Thus, an estimation of ice accretion should be carried out using other meteorological variables. Relevant literature [3]-[6] has shown that the estimation of ice accretion is a complicated procedure involving numerous parameters that are not easy to obtain, such as precipitation intensity and type, droplet collision efficiency, temperature etc. Herein the focus was on freezing rain events since those events cause ice to stick on the exposed surfaces of steel lattice towers and conductors, while snow events do not produce large ice accumulation; in general snow may stack on roofs but cannot easily stick as ice on tower members and conductors.

A simple ice accretion model for freezing rain events that requires easily available information is proposed by Jones [7]-[8]. According to the model, a uniform radial equivalent thickness R_{eq} (in mm) accumulating on a member of any cross-section during a precipitation event is estimated as:

$$R_{eq} = \frac{D}{S\rho_i}\sum_{j=1}^{N}\left[\left(P_j\rho_o\right)^2 + \left(3.6U_jW_j\right)^2\right]^{1/2} \qquad \text{Eq. 2.3}$$

where:

P_j is the precipitation rate (mm/hr), W_j is the liquid water content (mm/hr) calculated by the equation $W_j = 0.067P_j{}^{0.846}$, U_j is the wind speed (m/s), ρ_o is the density of water, ρ_i is the density of ice, D is the diameter of cross-section, S is the perimeter of cross-section and N is the duration of the event in hours.

Following Eq. (2.3) it is inferred that the estimation of accumulated ice mainly depends on wind speed, precipitation rate and the duration of the event, parameters that are easily available from weather stations. Furthermore, the estimation is valid regardless the shape of cross-section (e.g. circular, angle etc.). In case of a transmission line the interest is on circular cross-sections (for the conductors) and angle profiles (for the tower members). According to [7] the ratio D/S is equal to $1/\pi$ for all circular cross-sections and equal to $1/4$ for equal-leg angle profiles.

According to [4], a freezing rain event can occur if precipitation has fallen and the wet bulb temperature was lower than 0 ^{o}C. Thus, in order to specify the freezing rain events over the period of data, the wet-bulb temperature was estimated following the methodology provided by [9]. Finally, in the estimation of the thickness of ice layers it was assumed that ice starts melting when there is a consecutive period of 3hr or more with air temperature higher than 0 ^{o}C [5].

2.2.3 Joint Wind-Icing Hazard

The probability of occurrence of specific wind and ice thickness combinations is estimated by combining the distributions of wind speed (Section 2.2.1) and ice thickness (Section 2.2.2) and defining a joint wind and ice thickness distribution. A typical form of a joint wind and ice thickness distribution is shown in Figure 2.2.

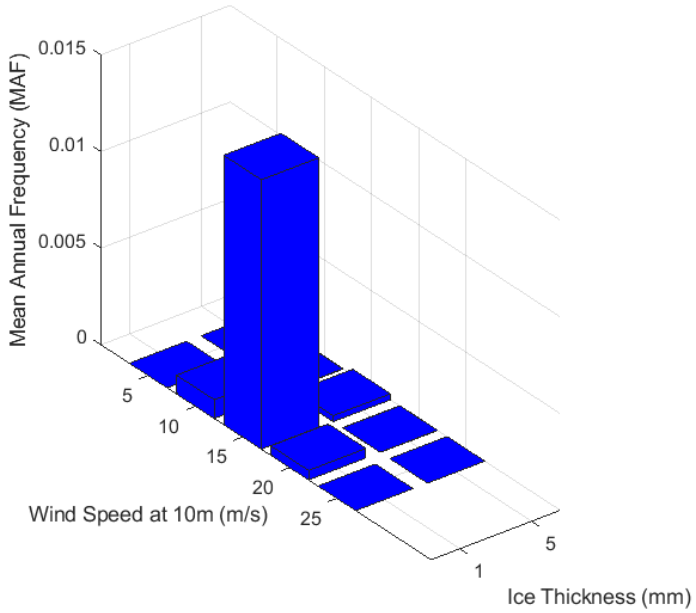

Figure 2.2: Typical form of Joint Wind and Ice Thickness distribution

2.3 Risk Estimation

The ultimate goal in a performance-based design is the estimation of the risk (of failure) of a specific structure given its structural strength and the hazard of its location. The probability of failure conditioned on the IM is specified by the fragility analysis as described in Section 2.1. The frequency of IM occurrence, or hazard is estimated following the process described in Section 2.2.

The combination of the information regarding fragility and hazard provides the risk of the structure. In other words, the risk, which is the probability of failure during the structure's service life, is estimated by integrating the structure's fragility function with the joint probability density function of wind and icing conditions:

$$\lambda = \int_{U=0}^{+\infty} \int_{R_{eq}=0}^{+\infty} P\left(D > C|U, R_{eq}\right) f\left(U, R_{eq}\right) \mathrm{d}U \, \mathrm{d}R_{eq} \qquad \text{Eq. 2.4}$$

where:

$P\left(D > C|U, R_{eq}\right)$ is the probability of failure (i.e. when demand D exceeds capacity C) for a given combination of wind speed U and ice thickness R_{eq} and it is actually provided by the fragility curve

of the structure, and $f(U, R_{eq})$ is the probability of occurrence of the combination of wind speed U and ice thickness R_{eq}, which corresponds to the hazard of the structure's location.

In order to account for the effect of wind direction Eq. (2.4) could be estimated for each of the wind directions (e.g. with wind angle θ) considered using the corresponding fragility curve. Then each value of $\lambda(\theta)$ is multiplied by the probability of occurrence of the corresponding wind direction $p(\theta)$ and finally the total probability λ is given by the equation:

$$\lambda = \sum_{\theta=1}^{n} p_\theta \lambda_\theta \qquad \text{Eq. 2.5}$$

The probability λ is usually an annualized probability of failure, thus the reciprocal of its value corresponds to the Return Period (RP) of failure in years:

$$RP = \frac{1}{\lambda} \qquad \text{Eq. 2.6}$$

Finally, the probability of failure during the service life of structure T can be estimated by the equation:

$$P_{fail} = 1 - e^{-\lambda T} \qquad \text{Eq. 2.7}$$

3 Case Study 1: Telecommunication Towers in Greece

The first type of lattice tower examined herein was a telecommunication tower. In specific, four different versions of a typical telecommunication tower were considered as presented in [10]. That type of tower is widely used by major telecommunication companies in Greece. For this reason, the estimation of risk of the aforementioned towers will refer to potential sites of installation in Greek territory.

For the estimation of risk of a structure two quantities are needed: the fragility of the structure and the hazard of its site. In the following, the application of the methodology of the risk assessment as presented in Section 2 will be applied to the case of the telecommunication towers in Greece.

3.1 Site Hazard

The first aspect for the evaluation of the risk of a structure is the estimation of the hazard of its site of installation. The hazard is site-specific (it depends only on the characteristics of the site and not on the structure) and in our case is related to the probability of (co-)occurrence of high wind speed and adverse ice conditions (large ice thickness accredited on surfaces).

The telecommunication towers of study referred to Greek practice and thus potential sites of installations throughout Greece were selected. Furthermore, the sites selected should be close to the shore, since the towers were designed for sites located to a distance less than 10Km from shore.

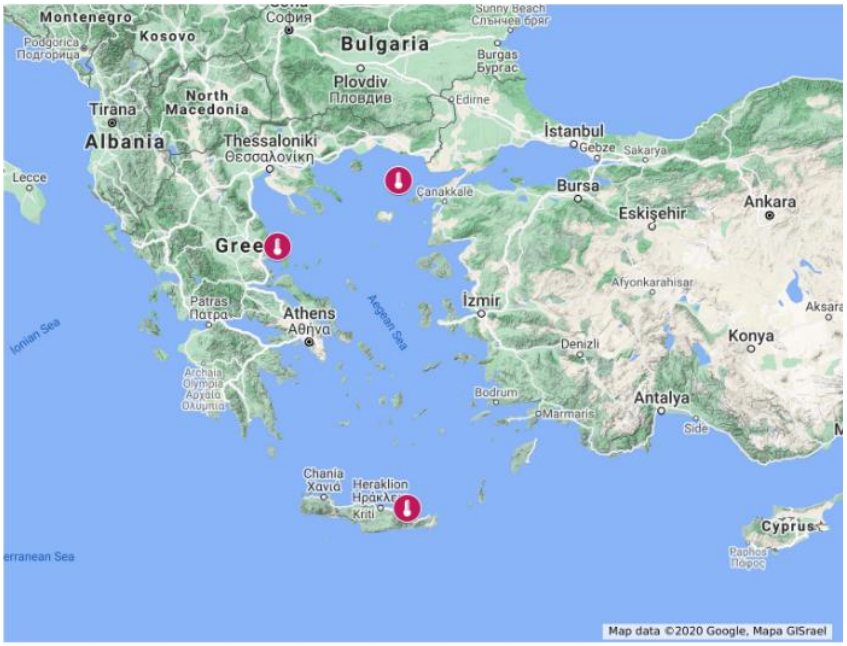

Figure 3.1: Sites of potential telecommunication tower installation in Greece

Figure 3.1 shows a map where the locations of the selected sites are annotated. In specific, three sites were selected: a) Samothraki (an island in North Aegean Sea), b) Zagora (a place located on the top of Mount Pelion in Central Greece) and c) Finokalia (a place located on the island of Crete in South Aegean Sea). All the sites met the proximity to the shore requirement and also showed different trends in their meteorological conditions. Finally, the corresponding meteorological data were obtained from weather stations installed in each site and administered by the National Observatory of Athens (NOA).

3.1.1 Samothraki

Figure 3.2 shows the wind speed distribution and the wind rose for the case of Samothraki in North Greece. Figure 3.2a shows the distribution of 10min Wind Speed at 10m height. It can be inferred that the majority of observations is lower than 5m/s. In addition, the mean wind speed observed was 3.63 m/s with a standard deviation of 3.49m/s. Finally, the probability of calm conditions was around 0.13. In terms of wind direction, the wind rose (Figure 3.2b) shows that the dominant wind direction is NNE (wind angle of 22.5°). Furthermore, high frequencies show the directions ENE (67.5°), SSE (157.5°) and SE (135°).

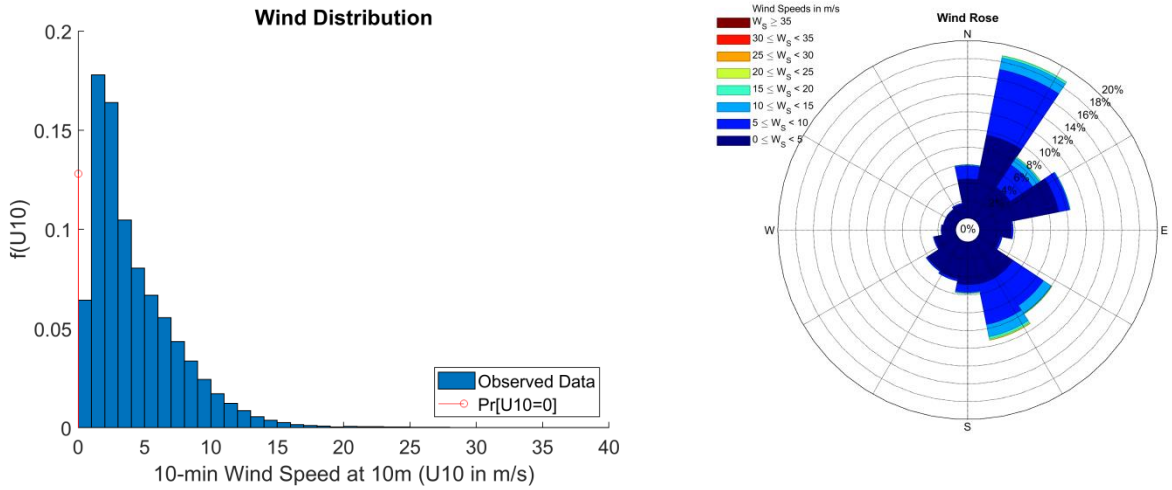

Figure 3.2: Distributions of a) Wind Speed and b) Wind Direction (Wind Rose) for Samothraki

In terms of the icing conditions due to the absence of measured data, the equivalent ice thickness R_{eq} was based on Eq. (2.3). Figure 3.3 shows the distribution of the resulted ice thicknesses. First of all, it is noteworthy that due to the climate of the site, ice has very low probability of observance (close to 0.5%). Thus, the probabilities of observing ice thicknesses different than 0 are very low (lower than 10^{-2}) as shown in Figure 3.3. Finally, the majority of ice thickness values is less than 1mm and the maximum one is less than 3mm.

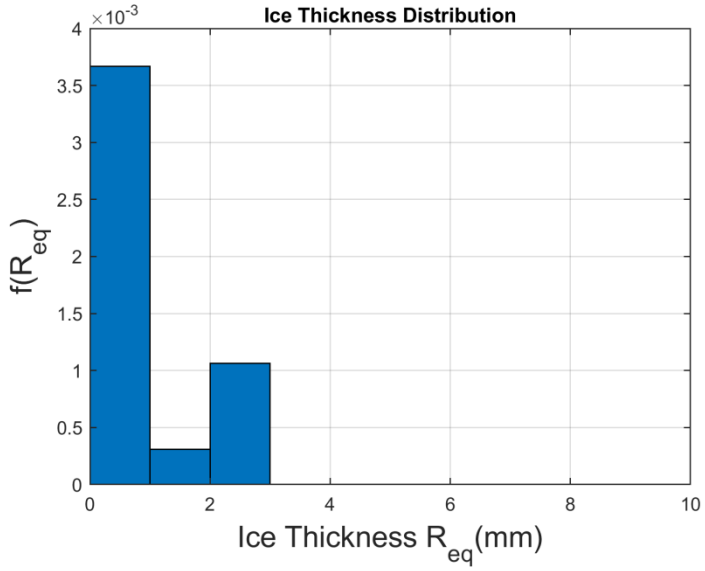

Figure 3.3: Distribution of Ice Thickness (R_{eq}) for Samothraki

The joint wind and ice thickness distribution is estimated by combining the distributions of wind speed (Figure 3.2a) and ice thickness (Figure 3.3). The result is given in Figure 3.4. During the estimation of the joint PDF, it was assumed that wind speed follows a Gumbel distribution while the ice thickness follows a lognormal distribution. Finally, it is noteworthy that the distribution of Figure 3.4 corresponds to cases when there is ice, thus the corresponding probabilities are low due to the low probability of ice.

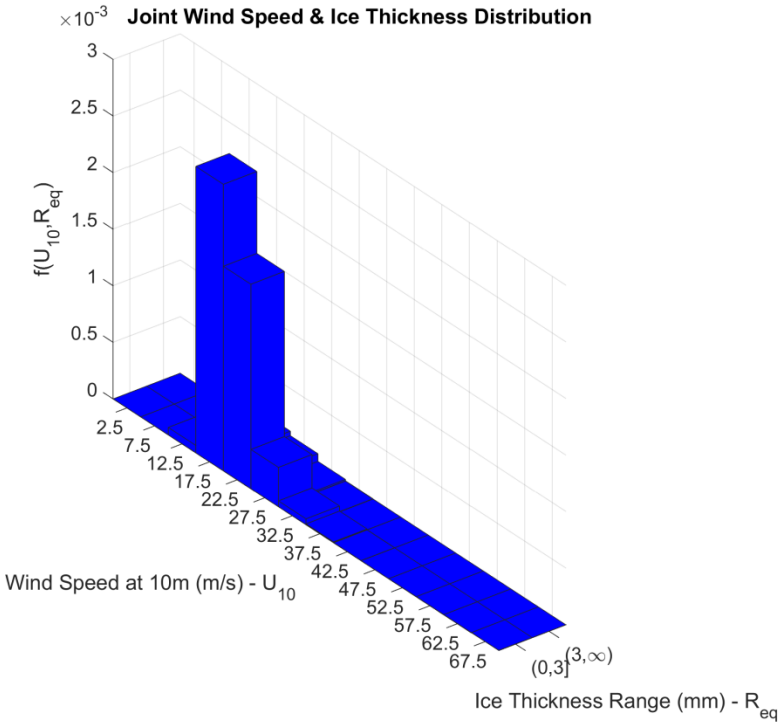

Figure 3.4: Joint Distribution of Wind Speed (U_{10}) and Ice Thickness (R_{eq}) for Samothraki

3.1.2 Zagora

Figure 3.5 shows the wind speed distribution and the wind rose for the case of Zagora on mount Pelion in Central Greece. According to Figure 3.5a, the site of Zagora is "less windy" than the site of Samothraki. In fact, the mean wind speed observed was 1.04 m/s with a standard deviation of 1.33m/s. Finally, the probability of calm conditions was around 0.34 (majority). In terms of wind direction, the wind rose (Figure 3.5b) shows that the dominant wind direction is W (wind angle of 270°). Furthermore, other directions especially related to west and east winds have significant frequencies.

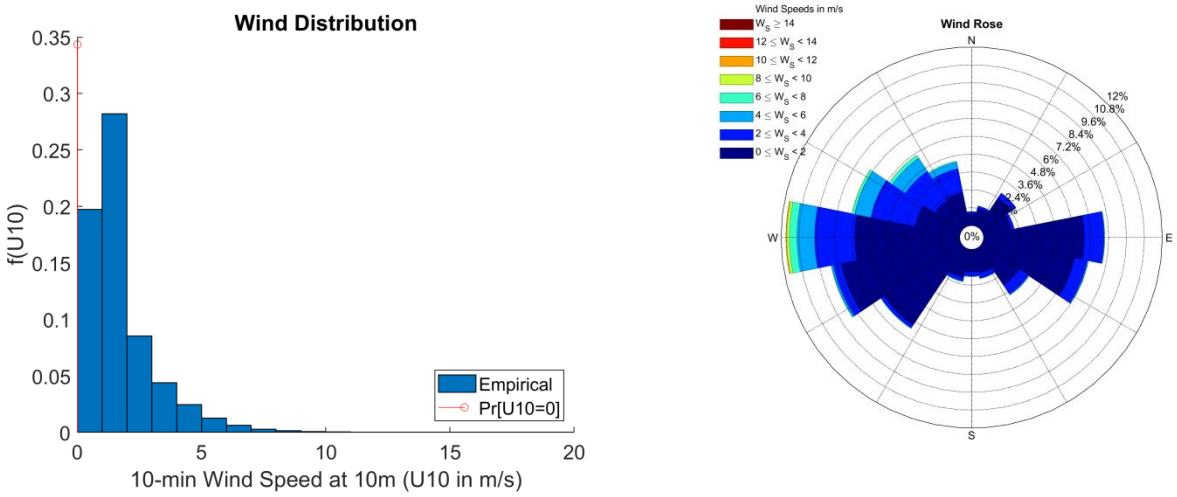

a) b)

Figure 3.5: Distributions of a) Wind Speed and b) Wind Direction (Wind Rose) for Zagora

Figure 3.6 shows the distribution of the ice thickness as estimated by Eq. (2.3). Due to the site geography (located on the top of a mountain), the probability of ice is larger than in the case of Samothraki. In fact, the estimated probability observing ice conditions was 1.55%. However, despite the larger probability of ice (as compared to Samothraki), the expected ice thicknesses are low and always lower than 4mm.

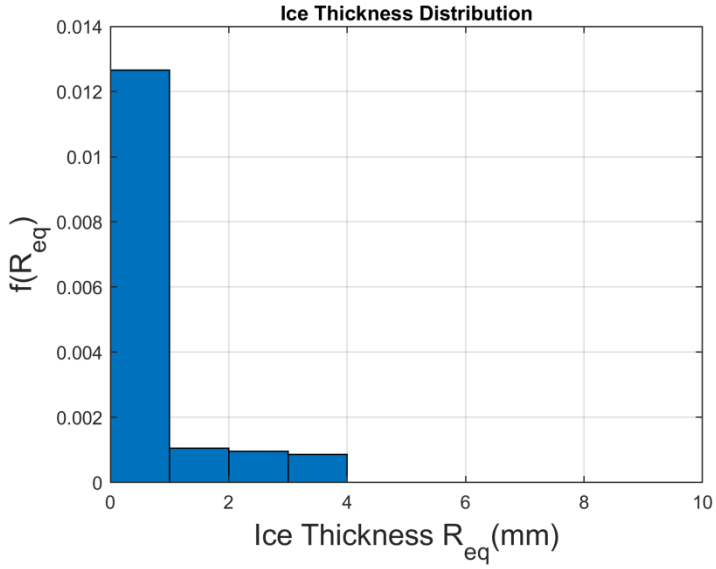

Figure 3.6: Distribution of Ice Thickness (R_{eq}) for Zagora

Figure 3.7 shows the joint wind and ice thickness distribution for the case of Zagora. Herein, the probabilities of combination of wind speed and ice thickness are larger than the case of Samothraki (Figure 3.4).

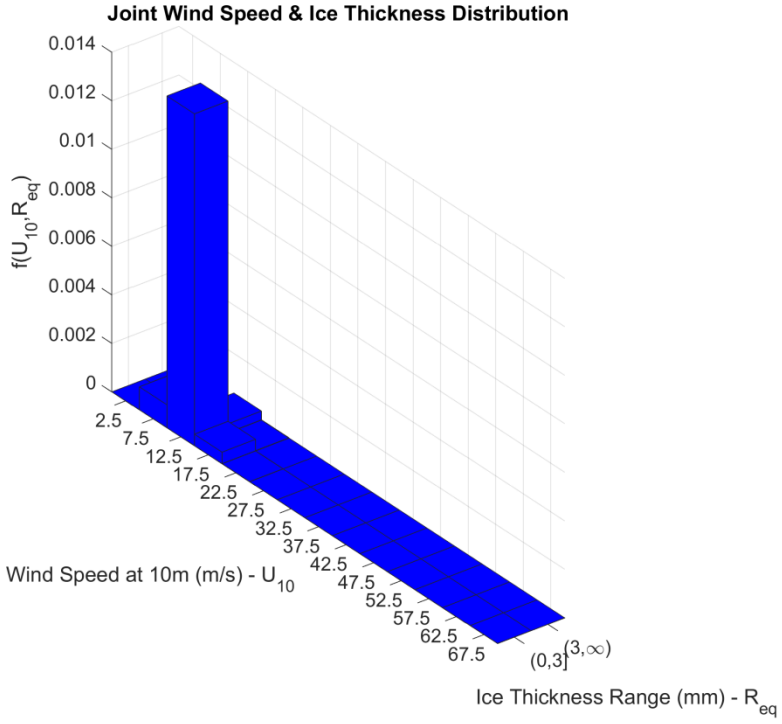

Figure 3.7: Joint Distribution of Wind Speed (U_{10}) and Ice Thickness (R_{eq}) for Zagora

3.1.3 Finokalia

Figure 3.8 shows the wind speed distribution and the wind rose for the case of Finokalia, a site located on the island of Crete in South Greece. According to Figure 3.8a, Finokalia is the "most windy" of the three selected sites. The mean wind speed was 7.71 m/s with a standard deviation of 4.69 m/s. Finally, the probability of calm conditions was really low (around 0.02), while high wind speeds with values larger than 30 m/s were observed. In terms of wind direction, the wind rose (Figure 3.8b) shows that the dominant wind direction is W (wind angle of 270°). Furthermore, only directions related to west winds seem to have significant frequencies.

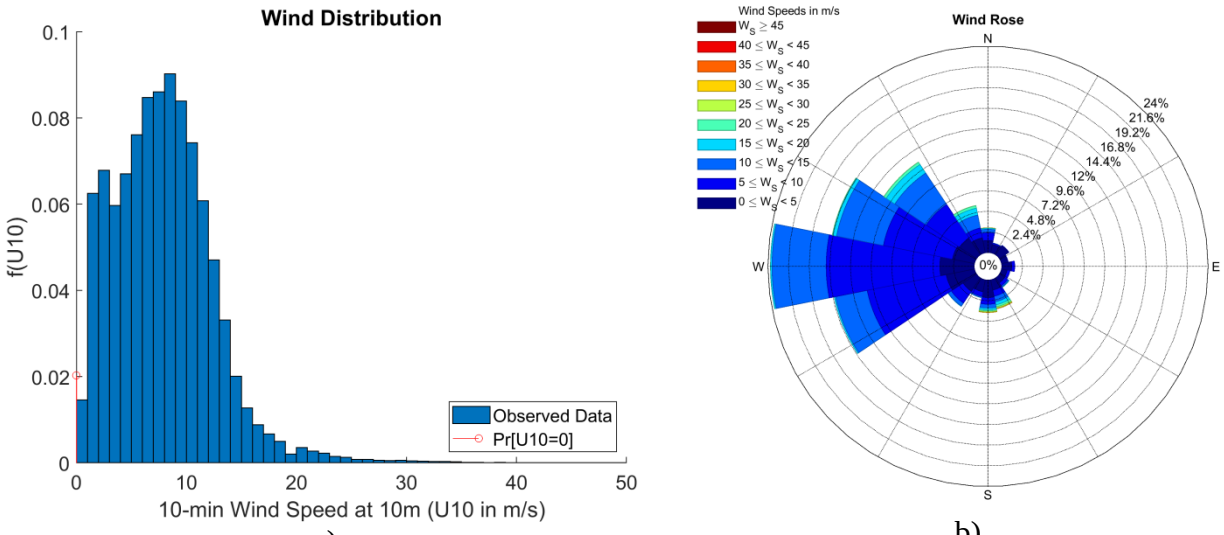

Figure 3.8: Distributions of a) Wind Speed and b) Wind Direction (Wind Rose) for Finokalia

As far as ice is concerned, the application of (Eq. 2.3) gave expected ice thickness equal to zero. So, any distribution of ice thickness could not be estimated. Thus, it is concluded that the hazard for the site of Finokalia is limited only to wind conditions, since ice seems to be negligible for that site.

All in all, the three sites selected for the estimation of risk of the telecommunication towers have different characteristics in terms of hazard. In specific, there are: a site with medium wind speed and low ice (Samothraki), a site with low wind speed and observable ice (Zagora) and finally a site with high wind speed and negligible ice (Finokalia). However, even in the case where ice is non-negligible the corresponding ice thicknesses are low making the wind as the governing hazard. The impact of the above cases of hazard on the risk of the various versions of telecommunication towers are presented in following Sections.

3.2 Risk of Initial Tower

The first version of the telecommunication tower was an initial design according to EN standards using conventional steel as presented in Section 2.4 of [10].

3.2.1 Tower's Fragility

The fragility of the tower was estimated following the methodology discussed in Section 2.1. For the estimation three scenarios of various ice thicknesses were examined (0mm, 1mm and 5mm) in combination with three scenarios of wind angle of attack (0°, 22.5° and 45°), resulting in nine different scenarios of ice thickness and wind angle of attack. It is noteworthy that the above scenarios are sufficient. First, as discussed in Section 3.1 the expected ice thickness is low, so there is no need for considering ice thicknesses larger than 5mm. Secondly, regarding the wind angle of attack, due to the tower's square cross-section, the three scenarios considered are sufficient to capture all the possible wind angles (directions) as shown in the wind roses.

For each of the aforementioned scenarios, a large number of non-linear dynamic analyses for a wide a range of wind speeds were performed and the corresponding probabilities of failure were estimated. At the end of the process, the parameters median θ and dispersion β of the fragility curve were estimated by using Eq. (2.1). Finally, the dispersion β was modified following Eq. (2.2).

Table 3.1 shows the parameters of the fragility curves for the nine scenarios considered regarding the initial design of the telecommunication tower. The corresponding fragility curves are depicted in Figure 3.9. It is observed that the median wind speed which corresponds to 50% probability of failure decreases as ice thickness increases. Certainly, this should be attributed to the fact that when ice accumulates on the structure's surfaces both the dead loads and the wind forces (due to the increase in the areas of projections) increase.

Table 3.1: Fragility parameters for the initial tower

Ice Thickness (mm)	Wind Angle 0°		Wind Angle 22.5°		Wind Angle 45°	
	Median (m/s)	Dispersion	Median (m/s)	Dispersion	Median (m/s)	Dispersion
0	38.00	0.0450	41.41	0.0400	45.41	0.0466
1	37.82	0.0459	41.39	0.0437	44.73	0.0445
5	37.02	0.0367	40.09	0.0478	44.54	0.0440
Mean Dispersion		0.0425		0.0438		0.0450
Total Dispersion		0.1179		0.1184		0.1189

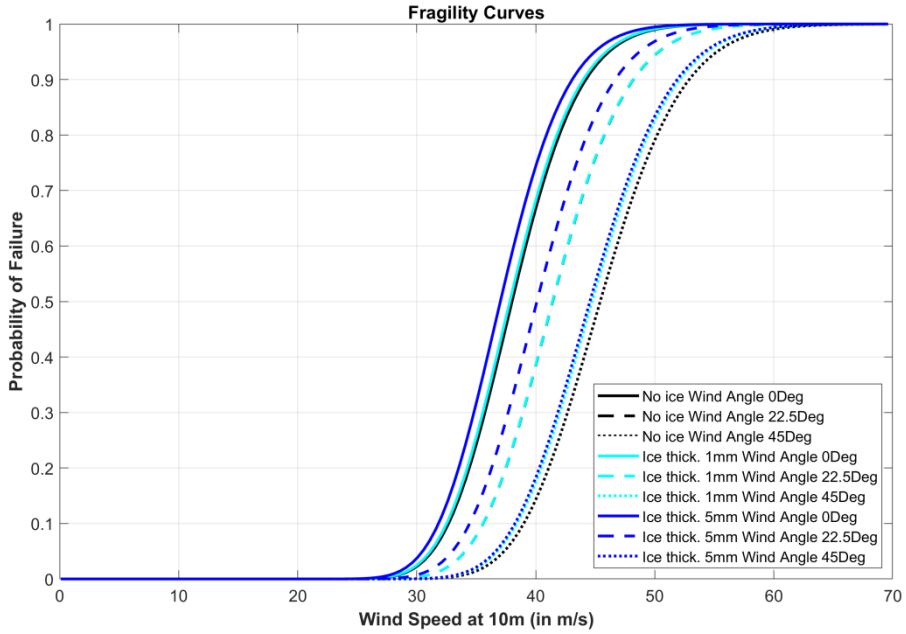

Figure 3.9: Fragility Curves for Initial Telecommunication Tower

3.2.2 Risk Estimation

The risk of the initial tower for each of the sites shown on Figure 3.1 can be easily estimated by combining the results of fragility (Section 3.2.1) and the estimated hazard (Section 3.1) following the methodology described in Section 2.3.

The annualized probability of failure λ is calculated by applying Eq. (2.4) for each of the wind directions considered. Then, based on the results of the wind rose, the corresponding probability of a wind direction is estimated and thus the total annualized probability of failure is calculated by applying Eq. (2.5). Finally, the corresponding Return Periods and the probability of failure during the service life of tower (e.g. 60 years) can be calculated by Eqs. (2.6) and (2.7).

Table 3.2 shows the results of the risk estimation for the initial tower for each of the potential sites of installation.

Table 3.2: Risk Estimation Results for the Initial Telecommunication Tower

Risk	Samothraki	Zagora	Finokalia
λ (yr^{-1})	6.29E-04	2.18E-09	0.31
Return Period (yrs)	1588.85	4.59E+08	3.18
Probability of Failure in 60yrs	0.037	1.31E-07	1.00

It is evident that the results follow the pattern of the hazard as described in Section 3.1. In specific, the largest probability of failure is observed for the site with the most adverse wind conditions (Finokalia). For that site the corresponding annualized probability of failure is $\lambda = 0.31$, a value that corresponds to a very short return period of 3.18 years. Thus, the probability of failure during the service life is equal to 1. This means that the specific type of tower is not suitable for that site.

For the rest of the two sites, the probabilities of failure are low and the return periods are high and, in any case, much higher than the assumed service life of the structure. Of course, as expected the site of Samothraki has larger probability of failure than the site of Zagora and this should be attributed to the higher wind conditions.

3.3 Risk of Corroded Tower

The second version of the telecommunication tower was a corroded version of the initial design. The assumptions for estimation of the corrosion effect and the resulting loss in structure members were presented in Section 2.5 of [10].

3.3.1 Tower's Fragility

Table 3.3 shows the parameters of the fragility curves for the nine scenarios considered as in the case of the initial tower. The corresponding fragility curves are depicted in Figure 3.10. In terms of the effect of ice thickness and the wind angle on the parameters, the findings are similar to those of the case of the initial tower (Table 3.1). However, it should be noted that all the median wind speeds are remarkably lower. This means that the corroded version of the tower is expected to fail in lower wind speeds than the initial tower. Certainly, this is reasonable and should be attributed to the lower strength of the corroded tower members due to the loss of steel (reduced cross-section thickness).

Table 3.3: Fragility Parameters for the Corroded Tower

Ice Thickness (mm)	Wind Angle 0°		Wind Angle 22.5°		Wind Angle 45°	
	Median (m/s)	Dispersion	Median (m/s)	Dispersion	Median (m/s)	Dispersion
0	33.98	0.0424	38.41	0.0479	45.41	0.0466
1	33.85	0.0400	36.30	0.0521	44.73	0.0445
5	32.50	0.0104	34.89	0.0414	44.54	0.0440
Mean Dispersion		0.0309		0.0471		0.0450
Total Dispersion		0.1143		0.1197		0.1189

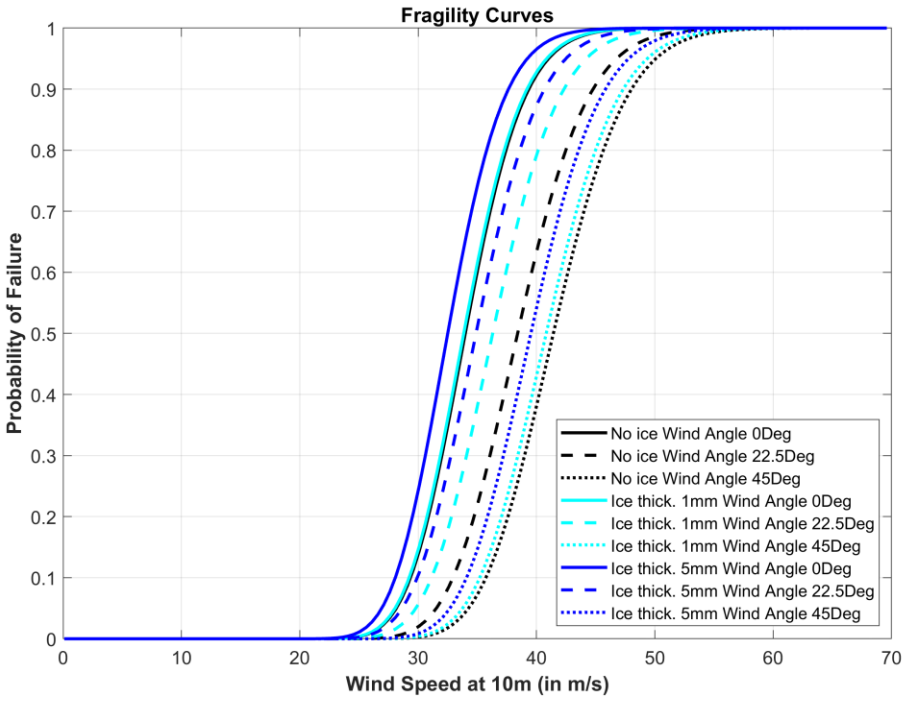

Figure 3.10: Fragility Curves for Corroded Telecommunication Tower

3.3.2 Risk Estimation

The risk of the corroded tower was estimated following the same process as in the case of the initial tower. The corresponding results for the three potential sites of installation are shown in Table 3.4.

Table 3.4: Risk Estimation Results for the Corroded Telecommunication Tower

Risk	Samothraki	Zagora	Finokalia
λ (yr^{-1})	1.98E-03	2.27E-08	0.45
Return Period (yrs)	504.13	4.41E+07	2.20
Probability of Failure in 60yrs	0.112	1.36E-06	1.00

The results of the risk estimation follow the same pattern as in the case of the initial tower (Table 3.2). However, for all sites the corresponding probabilities of failure are significantly higher (and the return periods lower). This finding should be attributed to the higher fragility of the corroded tower in comparison to the initial one.

3.4 Risk of Strengthened Hybrid Member Tower

The third version of the telecommunication tower was a strengthened version of the corroded tower with hybrid members strengthened via FRP plates. The methodology of strengthening was presented in Section 2.6 of [10].

3.4.1 Tower's Fragility

Table 3.5 shows the parameters of the fragility curves for the nine scenarios of ice thickness and wind angle combinations. The corresponding fragility curves are depicted in Figure 3.11. In terms of the effect of ice thickness and the wind angle on the parameters, the findings are similar to those of the cases of the initial and corroded towers. All the median wind speeds though fall between their corresponding values of the initial (Table 3.1) and the corroded tower (Table 3.3). This means that examined scenario of strengthening via FRP plates certainly increases the strength of the corroded tower but it is not sufficient to reach the strength of the initial tower.

Table 3.5: Fragility Parameters for the Strengthened Hybrid Member Tower

Ice Thickness (mm)	Wind Angle 0°		Wind Angle 22.5°		Wind Angle 45°	
	Median (m/s)	Dispersion	Median (m/s)	Dispersion	Median (m/s)	Dispersion
0	36.84	0.0349	39.98	0.0024	41.42	0.0034
1	36.84	0.0349	39.98	0.0024	40.04	0.0015
5	35.53	0.0545	38.38	0.0422	39.15	0.0303
Mean Dispersion		0.0414		0.0157		0.0117
Total Dispersion		0.1175		0.1111		0.1106

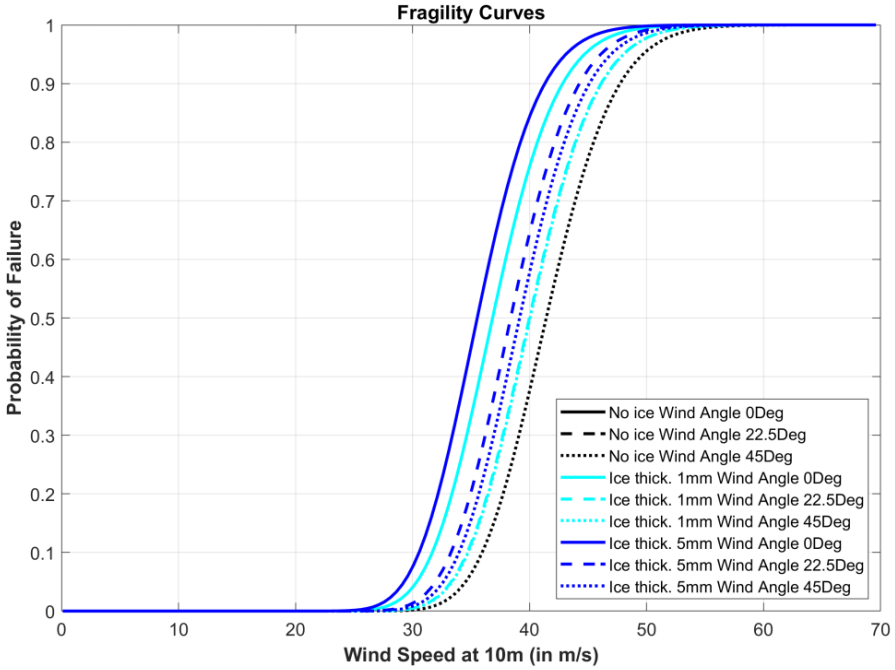

Figure 3.11: Fragility Curves for Strengthened Hybrid Member Telecommunication Tower

3.4.2 Risk Estimation

The results of the risk estimation for this version of tower are shown in Table 3.6.

Table 3.6: Risk Estimation Results for the Strengthened Hybrid Member Telecommunication Tower

Risk	Samothraki	Zagora	Finokalia
λ (yr^{-1})	9.57E-04	4.31E-09	0.38
Return Period (yrs)	1045.06	2.32E+08	2.66
Probability of Failure in 60yrs	0.056	2.59E-07	1.00

As expected, the results of the risk estimation when compared with those of the initial (Table 3.2) and corroded towers (Table 3.4) follow the same trend with the results of fragility. In other words, all the values fall between their corresponding values of corroded and initial versions.

3.5 Risk of High Strength Steel Tower

The fourth version of the telecommunication tower was a redesigned tower, having the same geometry with the initial tower, but with High Strength Steel (HSS) members. The specifications of the HSS version of the tower were presented in Section 2.7 of [10].

3.5.1 Tower's Fragility

Table 3.7 shows the parameters of the fragility curves for the nine scenarios of ice thickness and wind angle combinations. The corresponding fragility curves are depicted in Figure 3.12. In the case of HSS tower, the corresponding median wind speeds of failure are much larger than the initial model (Table 3.1). It is noteworthy that all the median wind speeds are larger than 40m/s. This finding should be attributed to the significant increase in the strength of the tower by using HSS and can show the benefit of using HSS instead of conventional steel.

Table 3.7: Fragility Parameters for the HSS Telecommunication Tower

Ice Thickness (mm)	Wind Angle 0°		Wind Angle 22.5°		Wind Angle 45°	
	Median (m/s)	Dispersion	Median (m/s)	Dispersion	Median (m/s)	Dispersion
0	41.99	0.0397	45.07	0.0078	47.94	0.0005
1	41.42	0.0338	45.27	0.0322	47.56	0.0008
5	40.82	0.0369	43.39	0.0373	46.62	0.0325
Mean Dispersion		0.0368		0.0258		0.0113
Total Dispersion		0.1160		0.1130		0.1106

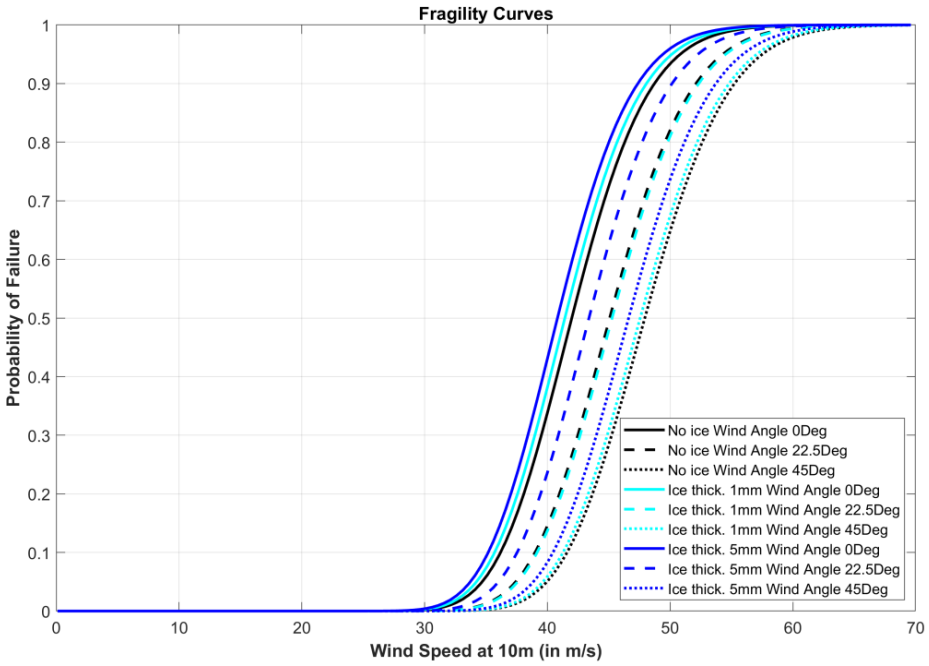

Figure 3.12: Fragility Curves for HSS Telecommunication Tower

3.5.2 Risk Estimation

The results of the risk estimation for the HSS telecommunication tower are shown in Table 3.8.

Table 3.8: Risk Estimation Results for the HSS Telecommunication Tower

Risk	Samothraki	Zagora	Finokalia
λ (yr^{-1})	1.73E-04	1.52E-10	0.20
Return Period (yrs)	5796.79	6.57E+09	4.97
Probability of Failure in 60yrs	0.0103	9.13E-09	0.999

As expected, the probabilities of failure are much lower in comparison with the rest of the models examined in this task. However, it is noteworthy that for the case of Finokalia even the use of HSS does not seem to reduce the probability of failure to a level that would exceed the service life of the structure.

4 Case Study 2: Suspension Transmission Towers in Germany

The second type of lattice tower was a power suspension transmission tower. The suspension tower followed the geometry of Danube tower, a type of transmission tower widely used in Central Europe. In specific three different versions of the tower (presented in [10]) were considered and their risk was estimated following a similar process as in the case of the telecommunication towers (Section 3).

For that cases of towers, the site of Annaberg-Buchholz was selected as a potential site of installation. This is located in Central-East Germany close to the borders with Czech Republic as shown on the map of Figure 4.1. Finally, the basic wind speed for the design of steel structures for that site is equal to 25 m/s according to the German national annex of Eurocodes.

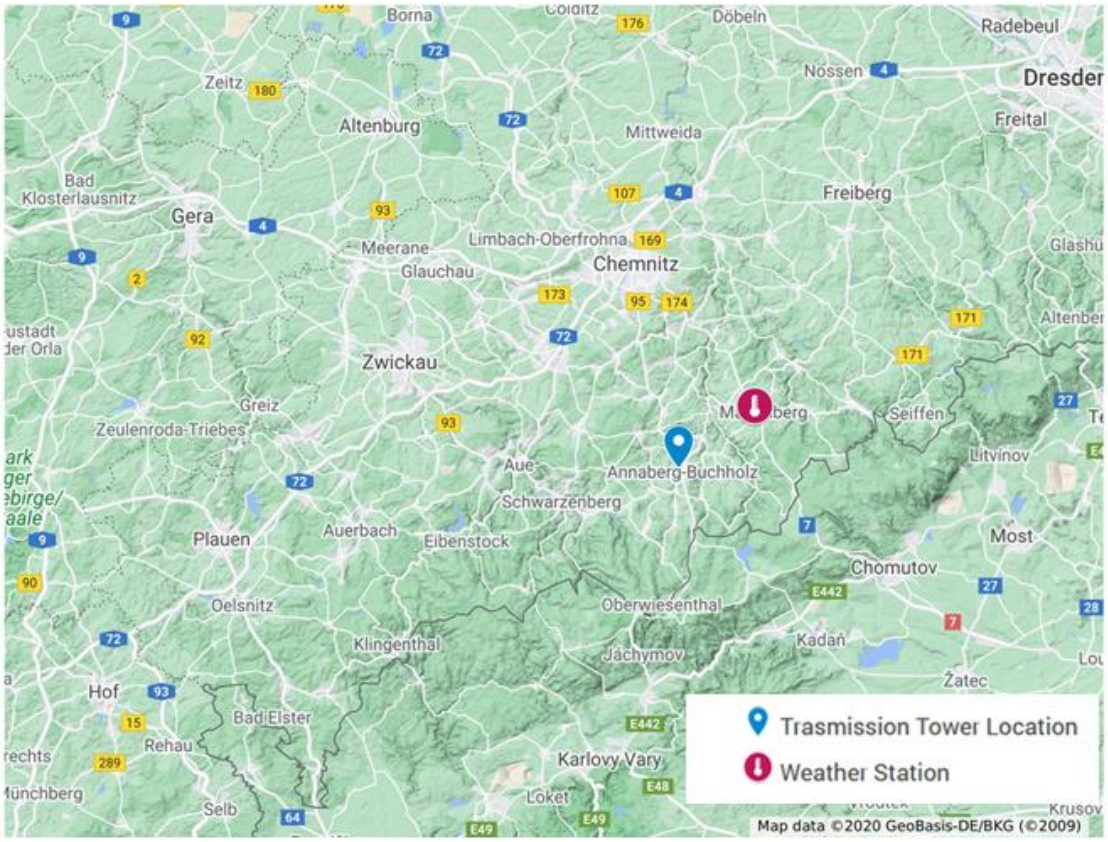

Figure 4.1: Site of transmission tower installation in Germany

4.1 Site Hazard

Following the methodology of risk assessment presented in previous sections, the first step for the evaluation of the risk of structure is the estimation of the hazard of the site of its location. The hazard was estimated based on meteorological data obtained from the closest weather station.

For the case of Annaberg -Buchholz, the closest weather station was located in Marienberg (Figure 4.1). The weather station of Marienberg is operated by the German Weather Service (Deutscher Wetterdienst – DWD) and provides detailed timeseries of various meteorological variables (wind speed and direction, air temperature, precipitation heights, etc.) for a long period of time.

4.1.1 Marienberg

Figure 4.2 shows the wind speed distribution and the wind rose for the site of Marienberg. Figure 4.2a shows the distribution of 10min Wind Speed at 10m height. It can be inferred that the majority of observations is lower than 5m/s. In addition, the mean wind speed observed was 2.96m/s with a standard deviation of 1.95m/s. Finally, the probability of calm conditions was around 4.34%. In terms of wind direction, the wind rose (Figure 4.2b) shows that the dominant wind direction is W (wind angle of 270°). Except of W, very high frequency (close to 20%) shows the direction SW (225°). All the rest of directions show frequencies less than 10% each.

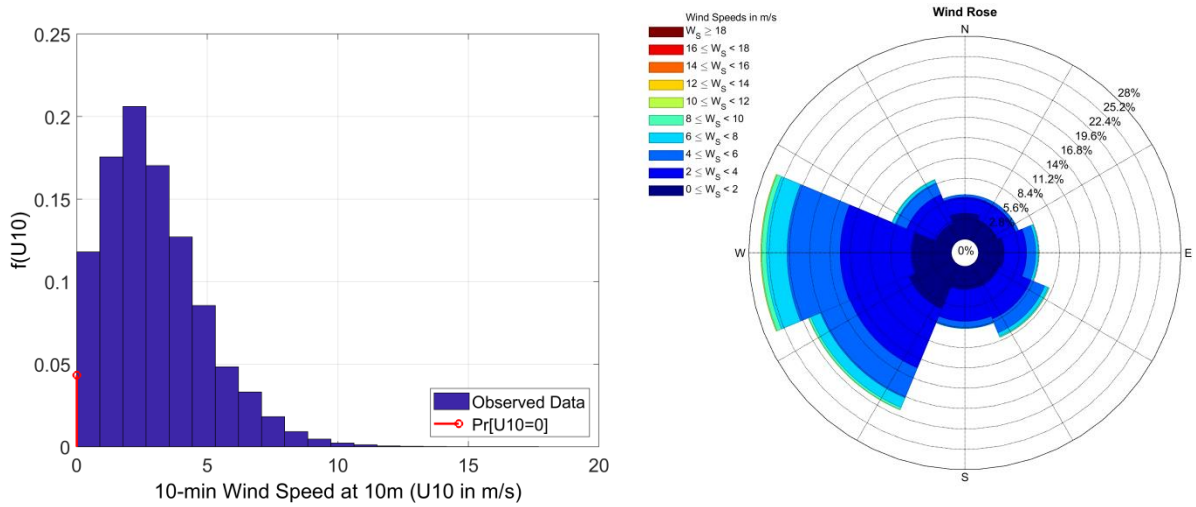

Figure 4.2: Distributions of a) Wind Speed and b) Wind Direction (Wind Rose) for Marienberg

In terms of the icing conditions due to the absence of measured data, the equivalent ice thickness R_{eq} was based on Eq. (2.3). First of all, from the statistical analysis of the resulted data the probability of ice conditions was estimated to be equal to 18.89%. This finding means that the potential site of the transmission towers installation has a non-negligible probability of ice conditions in contrast to the corresponding sites of the telecommunication towers (Section 3.1). Certainly, that should be attributed to the adverse climate of Central Germany as compared with that of Greece.

Figure 4.3 shows the distribution of the estimated ice thicknesses. It is noteworthy that the heights of the columns correspond to ice conditions (i.e. zero ice thickness was exported) which correspond to 18.89% of time. So, the values of z-axis were multiplied by 0.1889. It is observed that the vast majority of ice thickness was lower than 10mm, with a mean value of 5.86mm and a standard deviation of 7.35mm.

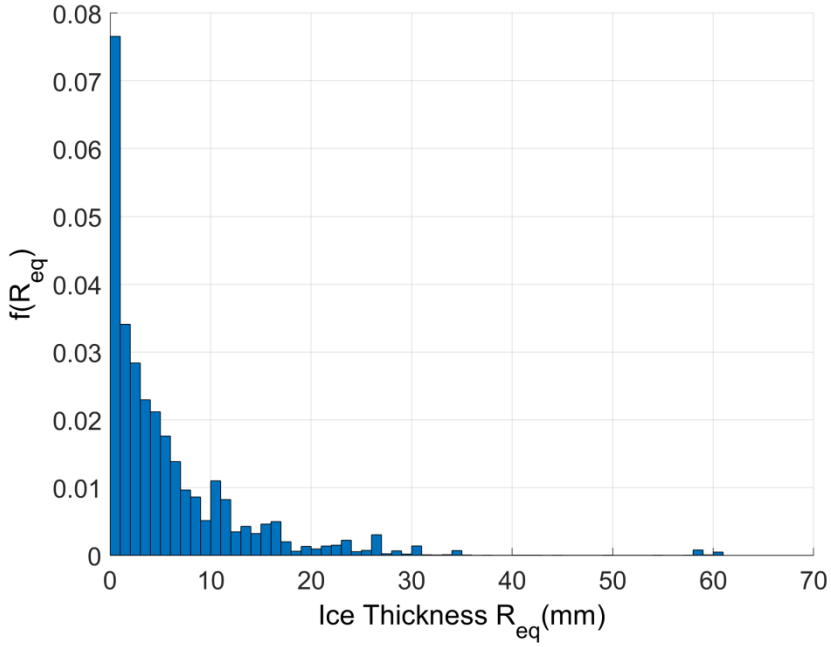

Figure 4.3: Distribution of Ice Thickness (R_{eq}) for Marienberg

The joint wind and ice thickness distribution is estimated by combining the distributions of wind speed (Figure 4.2a) and ice thickness (Figure 4.3). The result is given in Figure 4.4. During the estimation of the joint PDF, it was assumed that wind speed follows a Gumbel distribution while the ice thickness follows a lognormal distribution. Finally, it is noteworthy that the distribution corresponds to cases when there is ice (i.e. the values of z-axis are multiplied by 0.1889).

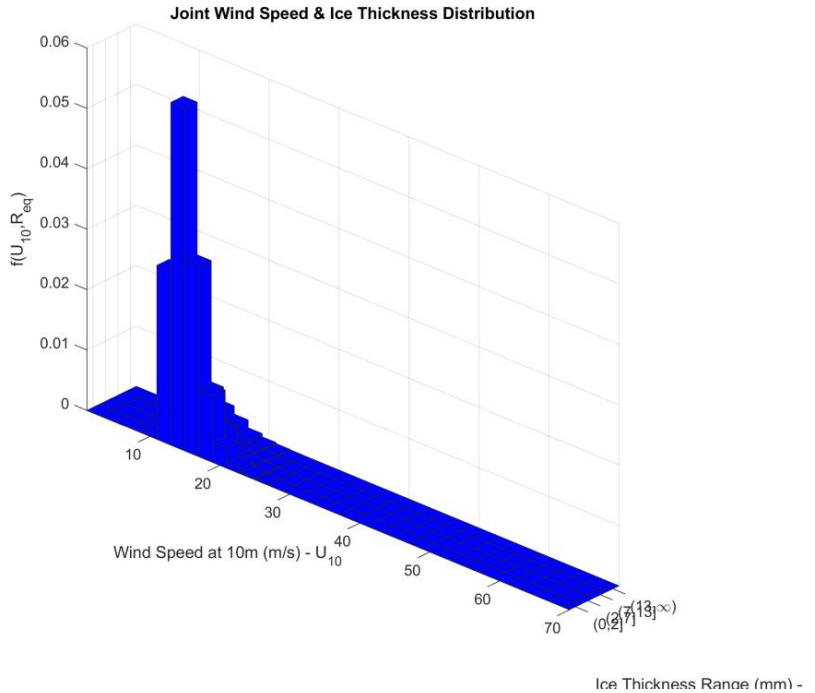

Figure 4.4: Joint Distribution of Wind Speed (U_{10}) and Ice Thickness (R_{eq}) for Marienberg

4.2 Risk of Initial Tower

The first version of the power suspension transmission tower was an initial design according to EN standards using conventional steel as presented in Section 3.3 of [10].

4.2.1 Tower's Fragility

The fragility of the suspension tower was estimated following the methodology discussed in Section 2.1 in similar way to the telecommunication towers. However, since more adverse icing conditions are expected more icing scenarios of larger thicknesses were considered. In specific, five scenarios of ice thicknesses were examined (0mm, 1mm, 5mm, 10mm and 15mm) in combination with three scenarios of wind angle of attack (0°, 45° and 90°), resulting in fifteen different scenarios of ice thickness and wind angle of attack.

Regarding the wind angle of attack, first the orientation of the tower (as part of a transmission line) was assumed to be N-S (Figure 4.5). Furthermore, due to tower's symmetry, the three scenarios of wind angle of attack considered herein are sufficient to capture all the possible wind angles (directions) as shown in the wind roses. In terms of notation, a wind angle of 0° (i.e. wind of North direction) was considered to be longitudinal to the line while a wind angle of 90° (i.e. wind of East direction) was considered to be transversal to the line.

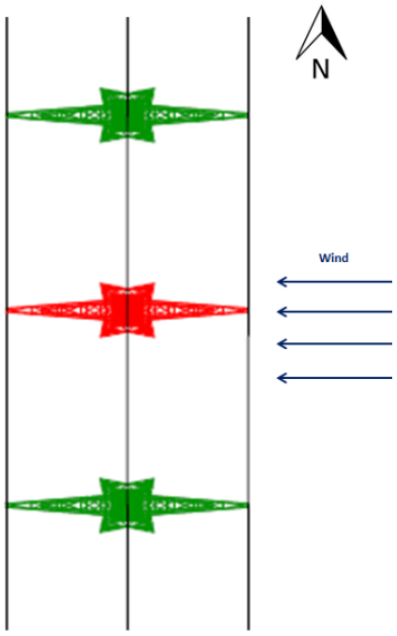

Figure 4.5: Power line (and Transmission Towers) orientation

For each of the fifteen scenarios, a large number of non-linear dynamic analyses for a wide a range of wind speeds were performed and the corresponding probabilities of failure were estimated. At the end of the process, the parameters median θ and dispersion β of the fragility curve were estimated by using Eq. (2.1). Finally, the dispersion β was modified following Eq. (2.2).

Table 4.1 shows the parameters of the fragility curves for the fifteen scenarios considered regarding the initial design of the power suspension transmission tower. The corresponding fragility curves are depicted in Figure 4.6 through Figure 4.8. The fragility curves follow a similar pattern to that of the telecommunication towers with the median wind speed to decrease as ice thickness increases. Furthermore, the wind with direction transversal to the line seems to be the most adverse case since it corresponds to lower median wind speeds of failure.

Table 4.1: Fragility Parameters for the Initial Suspension Tower

Ice Thickness (mm)	Wind Angle 90°		Wind Angle 45°		Wind Angle 0°	
	Median (m/s)	Dispersion	Median (m/s)	Dispersion	Median (m/s)	Dispersion
0	29.64	0.0240	32.21	0.0339	30.74	0.0277
1	28.41	0.0197	31.35	0.0414	30.59	0.0339
5	25.03	0.0056	28.96	0.0058	29.38	0.0277
10	21.81	0.0248	25.49	0.0196	26.12	0.0307
15	19.66	0.0241	23.45	0.0335	21.92	0.0466
Mean Dispersion		0.0196		0.0269		0.0333
Total Dispersion		0.1117		0.1132		0.1149

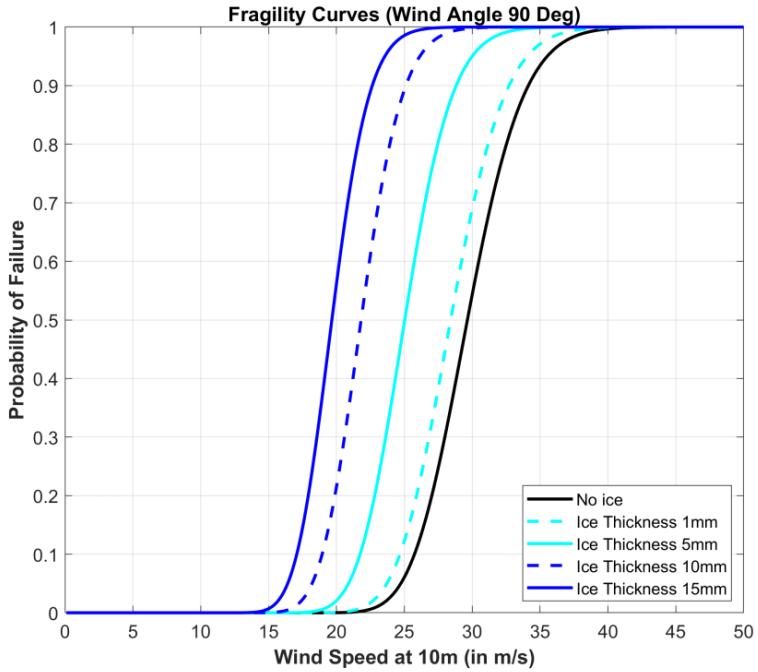

Figure 4.6: Fragility curves for Initial Suspension Tower and Wind Angle Transversal to the line

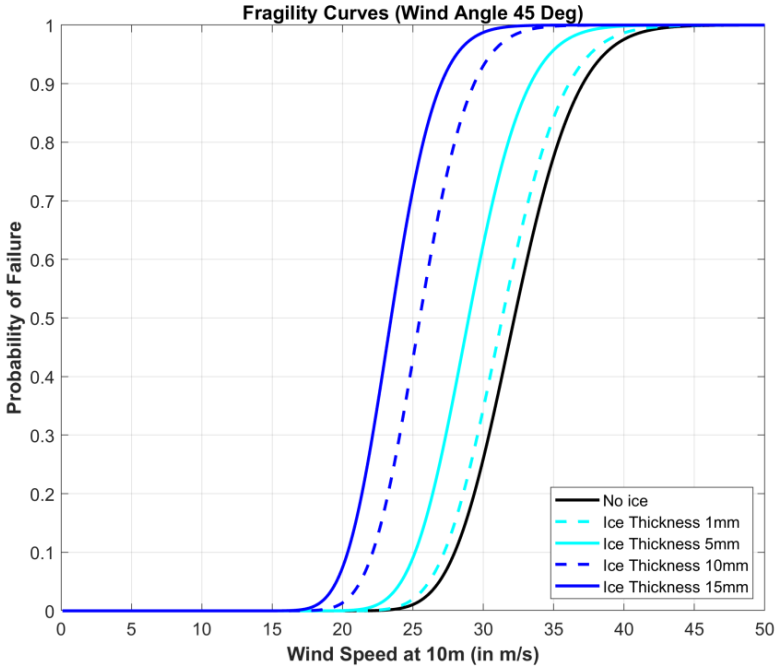

Figure 4.7: Fragility curves for Initial Suspension Tower and Wind Angle of 45 Degrees

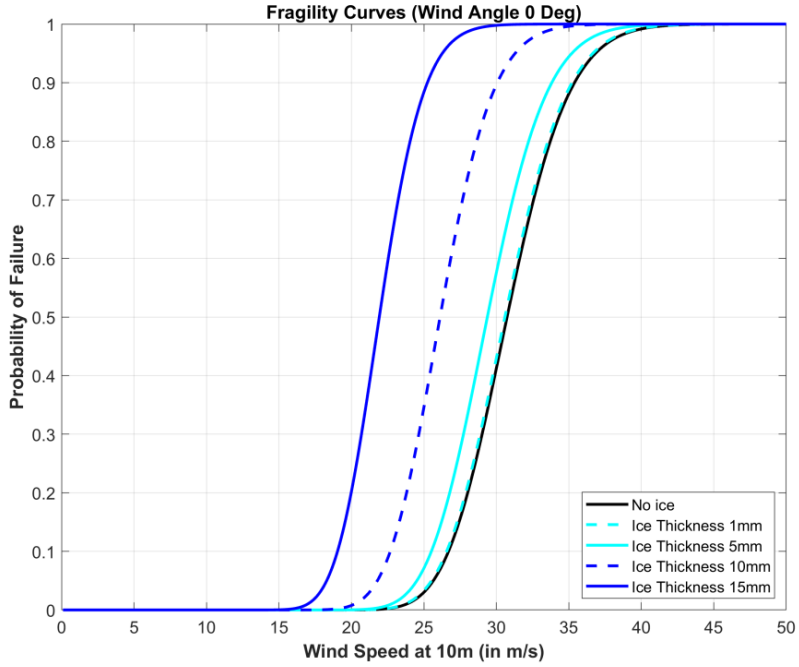

Figure 4.8: Fragility curves for Initial Suspension Tower and Wind longitudinal to the line

4.2.2 Risk Estimation

The risk of the initial tower can be easily estimated by combining the results of fragility (Section 4.2.1) and the corresponding site hazard (Section 4.1) following the methodology described in Section 2.3.

The annualized probability of failure λ is calculated by applying Eq. (2.4) for each of the wind directions considered. Then, based on the results of the wind rose, the corresponding probability of a wind direction is estimated and thus the total annualized probability of failure is calculated by

applying Eq. (2.5). Finally, the corresponding Return Periods and the probability of failure during the service life of tower (e.g. 60 years) can be calculated by Eqs. (2.6) and (2.7).

Table 4.2 shows the results of the risk estimation for the initial tower for the selected site of installation.

Table 4.2: Risk Estimation Results for the Initial Suspension Transmission Tower

Risk	Annaberg -Buchholz
λ (yr^{-1})	1.84E-04
Return Period (yrs)	5435.97
Probability of Failure in 60yrs	0.0110

It is evident that the combination of the structure's characteristics and the hazard of its location corresponds to a low annualized probability of failure and a high return period. Finally, the estimated probability of failure during tower's service life (which is assumed to be 60 years) is 0.011.

4.3 Risk of Corroded Tower

The second version of the suspension transmission tower was a corroded version of the initial tower. The assumptions for estimation of the corrosion effect and the resulting loss in structure members were presented in Section 3.4 of [10].

4.3.1 Tower's Fragility

Table 4.3 shows the parameters of the fragility curves for the fifteen scenarios considered as in the case of the initial tower following the same assumptions in terms of the tower orientation. The corresponding fragility curves are depicted in Figure 4.9 through Figure 4.11. In terms of the effect of ice thickness and the wind angle on the parameters, the findings are similar to those of the case of the initial tower (Table 4.1). However, it should be noted that similarly to the case of the corroded telecommunication tower, all the median wind speeds are remarkably lower. This means that the corroded version of the tower is expected to fail in lower wind speeds than the initial tower. This finding should be attributed to the lower strength of the corroded tower members due to the loss of steel (reduced cross-section thickness).

Table 4.3: Fragility Parameters for the Corroded Suspension Tower

Ice Thickness (mm)	Wind Angle 90°		Wind Angle 45°		Wind Angle 0°	
	Median (m/s)	Dispersion	Median (m/s)	Dispersion	Median (m/s)	Dispersion
0	27.33	0.0296	29.03	0.0047	26.92	0.0259
1	25.66	0.0185	28.01	0.0343	26.50	0.0395
5	22.11	0.0363	25.93	0.0064	26.04	0.0040
10	19.86	0.0072	23.02	0.0247	22.95	0.0416
15	17.17	0.0312	20.57	0.0272	17.56	0.0383
Mean Dispersion		0.0246		0.0195		0.0299
Total Dispersion		0.1127		0.1117		0.1140

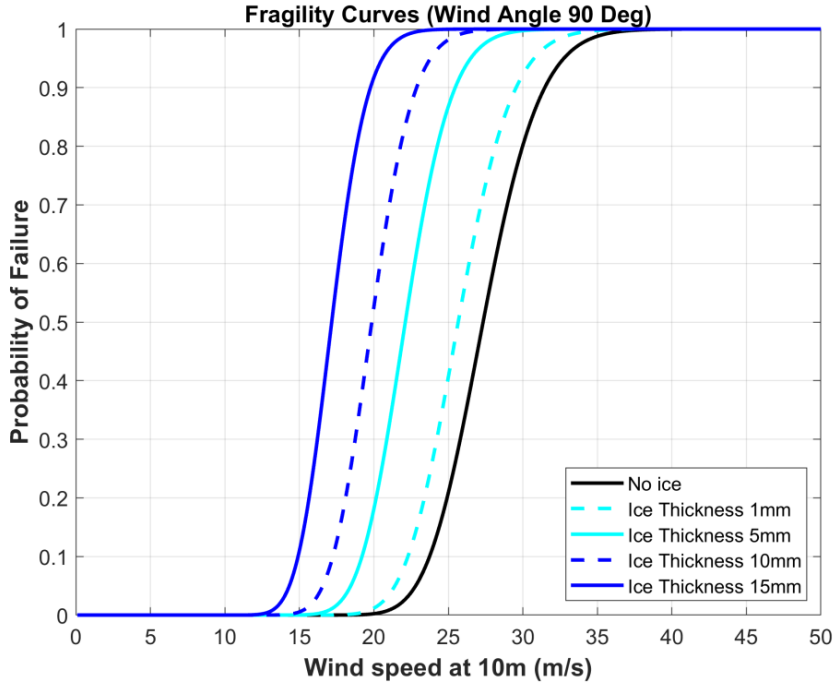

Figure 4.9: Fragility curves for Corroded Suspension Tower and Wind Angle Transversal to the line

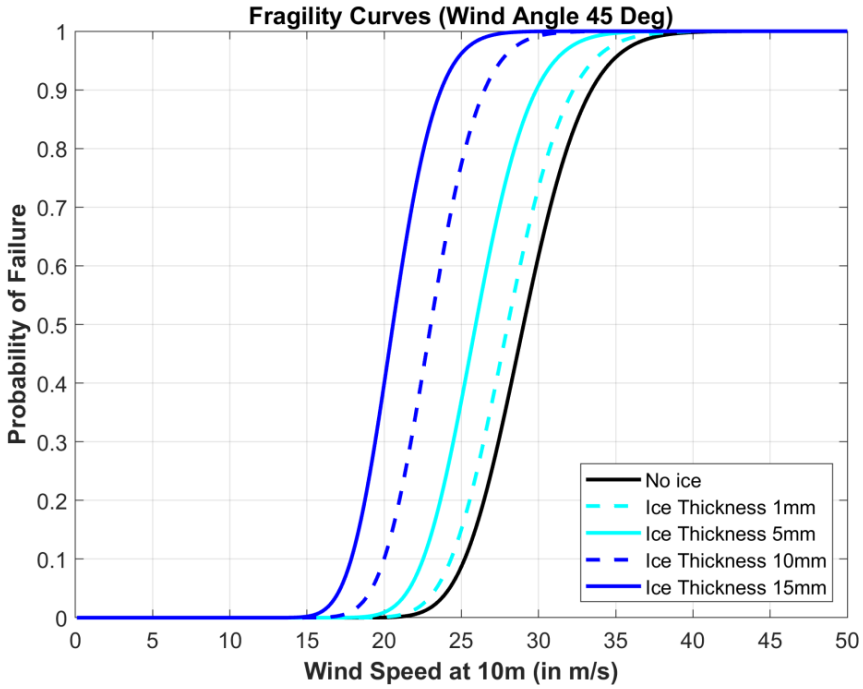

Figure 4.10: Fragility curves for Corroded Suspension Tower and Wind Angle of 45 Degrees

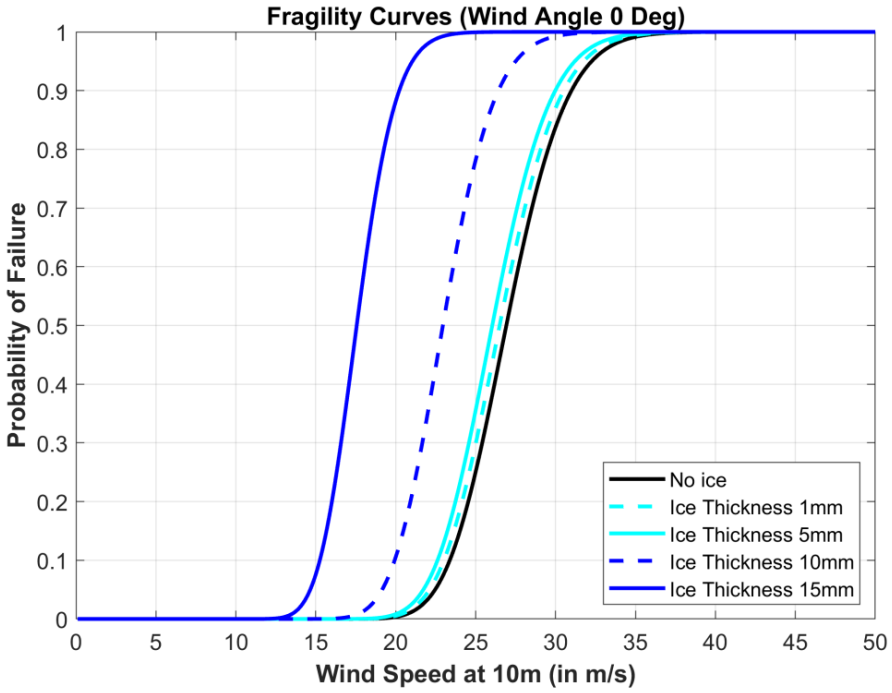

Figure 4.11: Fragility curves Corroded Suspension Tower and Wind longitudinal to the line

4.3.2 Risk Estimation

The risk of the corroded tower was estimated following the same process as in the case of the initial tower. The corresponding results are shown in Table 4.4.

Table 4.4: Risk Estimation Results for the Corroded Suspension Transmission Tower

Risk	Annaberg -Buchholz
λ (yr^{-1})	7.37E-04
Return Period (yrs)	1357.08
Probability of Failure in 60yrs	0.0432

It is observed that the corresponding probability of failure is higher (and the return period lower). This finding should be attributed to the higher fragility of the corroded tower in comparison to the initial one. Nevertheless, even a corroded version of the tower seems to have only 4.3% probability of failure during the 60 years of its service life.

4.4 Risk of High Strength Steel Tower

The last version of the suspension transmission tower was a redesigned tower, having the same geometry with the initial tower, but with High Strength Steel (HSS) members. The specifications of the HSS version of the tower were presented in Section 3.5 of [10].

4.4.1 Tower's Fragility

Table 4.5 shows the parameters of the fragility curves for the fifteen scenarios of ice thickness and wind angle combinations. The corresponding fragility curves are depicted in Figure 4.12 through

Figure 4.14. In the case of HSS tower, the corresponding median wind speeds of failure are close to the case of the initial model (Table 4.1). This is an interesting finding especially when it is combined with the fact that using HSS members resulted in a lighter structure by about 1.0 ton. So, despite the lighter structure, the resulting strength is almost the same with that of the initial design with conventional steel. Thus, an important inference is that by using HSS members the same strength may be achieved but at lower cost (weight of structure).

Table 4.5: Fragility Parameters for the HSS Suspension Tower

Ice Thickness (mm)	Wind Angle 90°		Wind Angle 45°		Wind Angle 0°	
	Median (m/s)	Dispersion	Median (m/s)	Dispersion	Median (m/s)	Dispersion
0	29.57	0.0189	30.49	0.0267	31.35	0.0316
1	28.33	0.0166	29.63	0.0321	30.49	0.0238
5	24.59	0.0327	27.48	0.0372	29.05	0.0402
10	21.03	0.0277	24.41	0.0173	25.72	0.0290
15	18.57	0.0302	22.18	0.0298	21.33	0.0221
Mean Dispersion		0.0252		0.0286		0.0293
Total Dispersion		0.1129		0.1137		0.1138

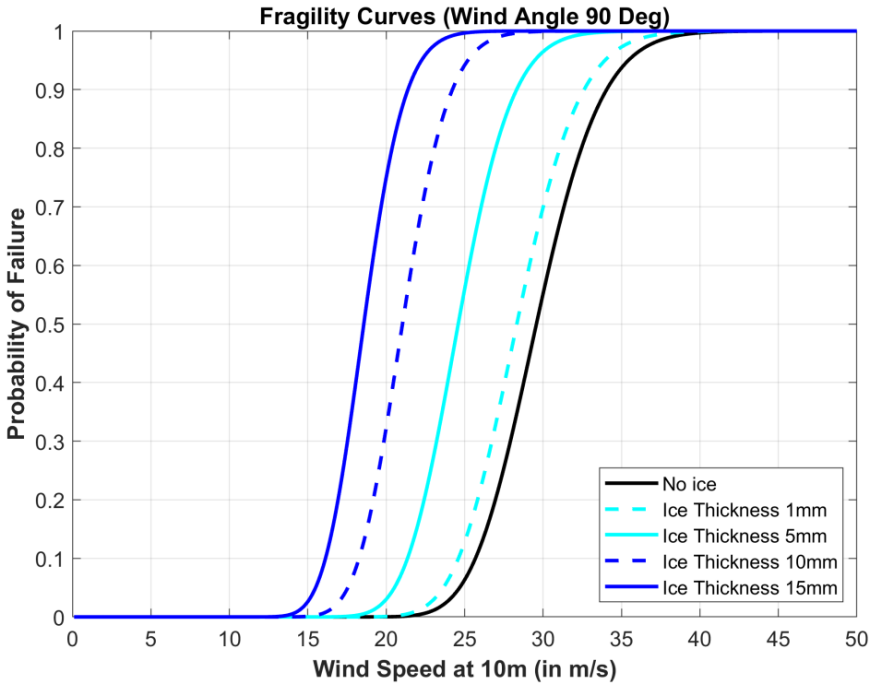

Figure 4.12: Fragility curves for HSS Suspension Tower and Wind Angle Transversal to the line

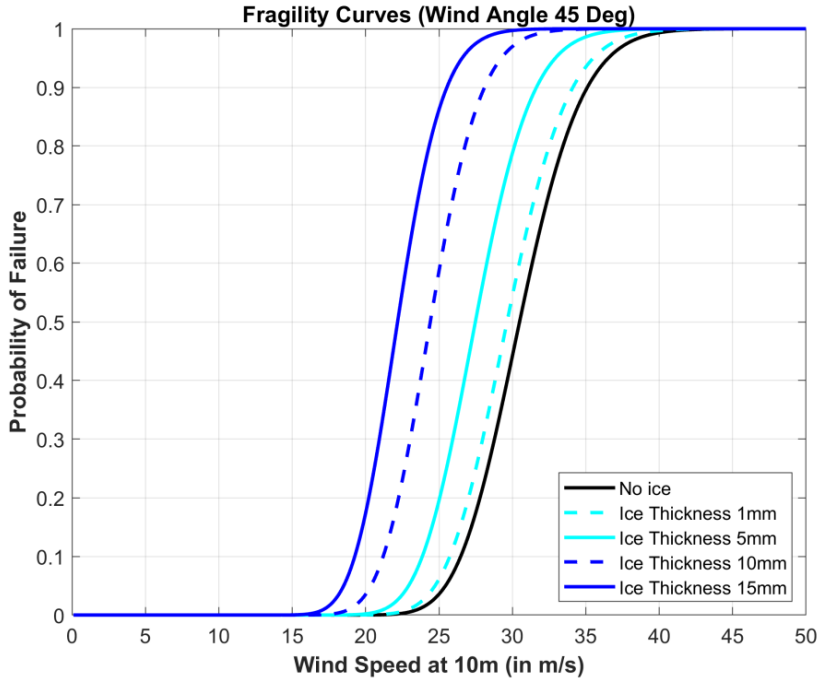

Figure 4.13: Fragility curves for HSS Suspension Tower and Wind Angle of 45 Degrees

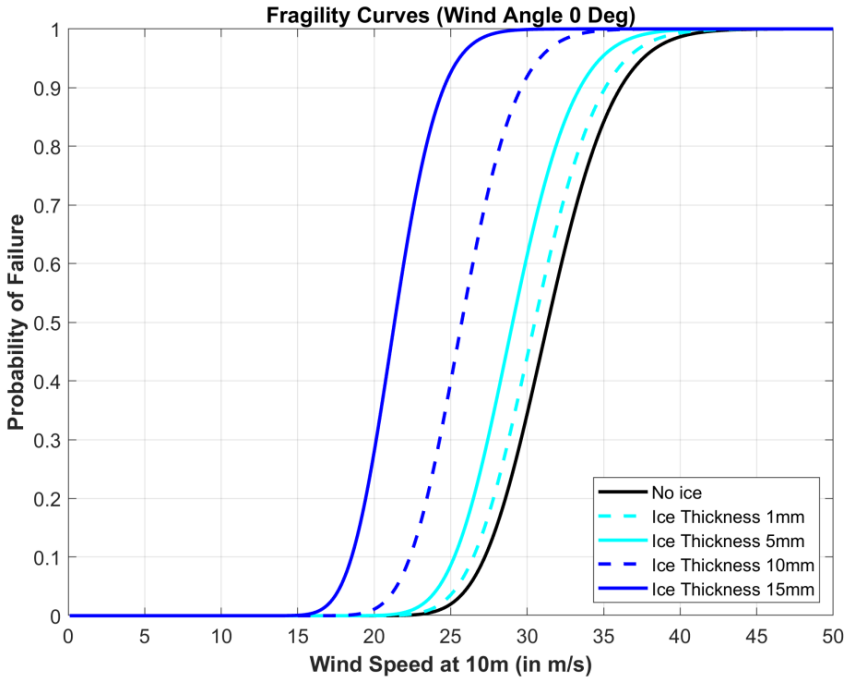

Figure 4.14: Fragility curves for HSS Suspension Tower and Wind longitudinal to the line

4.4.2 Risk Estimation

The results of the risk estimation for the HSS suspension transmission tower are shown in Table 4.6.

Table 4.6: Risk Estimation Results for the HSS Suspension Transmission Tower

Risk	Annaberg -Buchholz
λ (yr^{-1})	2.83E-04
Return Period (yrs)	3536.80
Probability of Failure in 60yrs	0.0168

As expected, the probability of failure is much lower in comparison with the corroded tower and close to that of the initial design. In specific, the HSS suspension tower of study has a probability of failure equal to 1.68% during its service life which is comparable with the 1.10% of the initial design with conventional steel.

5 Case Study 3: Dead-End Transmission Towers in Germany

The third type of lattice tower considered herein was a Dead-End transmission tower. Dead-End towers constitute important parts of a power transmission line. They differ from the suspension tower since they are capable of carrying the longitudinal loads of the conductors, while the suspension towers carry only vertical loads.

Herein a Dead-End transmission tower of the same geometry with the suspension tower was considered. The risk of that tower was estimated for the same location with the suspension tower (same hazard) and for four different versions of the tower as presented in Section 4 of [10].

The risk of the Dead-End transmission towers was estimated following exactly the same procedure as in the case of the suspension towers (Section 4).

5.1 Site Hazard

Since the location of the Dead-End transmission tower is the same with that of the suspension tower (i.e. both can be considered parts of the same power line), the hazard of the site does not differ and its estimation is described in Section 4.1.

5.2 Risk of Initial Design Tower

The first version of the power Dead-End transmission tower was an initial design according to EN standards using conventional steel as presented in Section 4.3 of [10].

5.2.1 Tower's Fragility

For the estimation of fragility, the same fifteen different scenarios of ice thickness and wind angle of attack and the same assumptions about the orientation of the tower were made as described in Section 4.2.1.

Table 5.1 shows the parameters of the fragility curves for the fifteen scenarios considered regarding the initial design of the Dead-End transmission tower. The corresponding fragility curves are depicted in Figure 5.1 through Figure 5.3. The fragility curves follow a similar pattern to that of the suspension tower with the median wind speed to decrease as ice thickness increases.

The values of median wind speeds of failure for each wind and icing combination are much larger than the corresponding wind speeds of the suspension tower. This certainly should be attributed to the larger strength of the Dead-End tower in order to carry larger loads (longitudinal plus vertical) than the suspension tower.

Regarding the wind angle of attack, results show a reverse effect as compared with the suspension tower. In specific the lowest median wind speed is observed when the wind direction is longitudinal to the line (and not transversal). However, the values of median wind speed of failure are still much larger than the corresponding values (and the transversal) of the suspension tower. A possible explanation could be that a large wind speed value along the power line will cause the failure of the cross-arms first (and not the body of the tower) and thus the Dead-End tower is expected to fail in lower wind speeds in the longitudinal direction than the transversal one.

Table 5.1: Fragility Parameters for the Initial Dead-End Tower

Ice Thickness (mm)	Wind Angle 90°		Wind Angle 45°		Wind Angle 0°	
	Median (m/s)	Dispersion	Median (m/s)	Dispersion	Median (m/s)	Dispersion
0	62.06	0.0022	54.00	0.0280	40.60	0.0345
1	60.34	0.0159	52.51	0.0300	39.48	0.0355
5	54.45	0.0199	47.38	0.0330	35.63	0.0335
10	47.68	0.0209	41.49	0.0350	31.19	0.0355
15	43.10	0.0164	37.51	0.0360	28.20	0.0365
Mean Dispersion		0.0151		0.0324		0.0351
Total Dispersion		0.1110		0.1147		0.1155

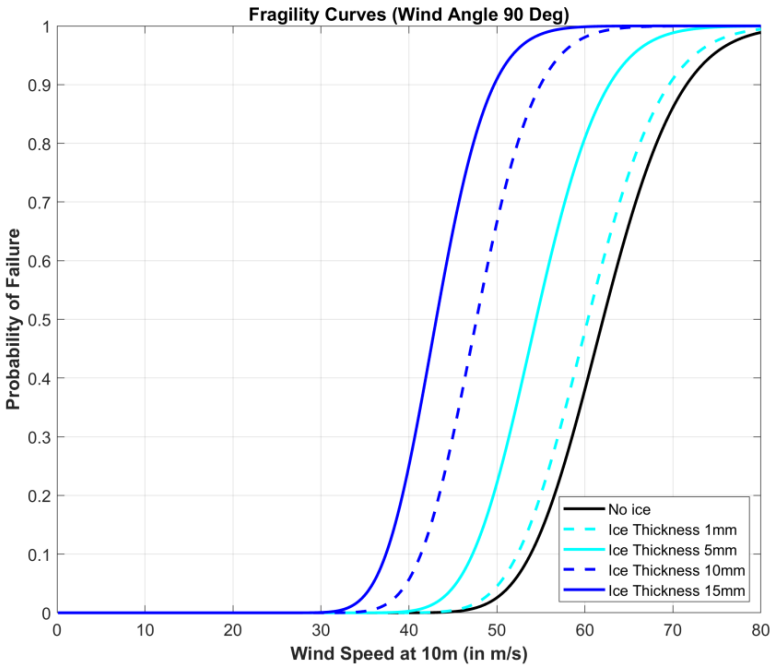

Figure 5.1: Fragility curves for Initial Dead-End Tower and Wind Angle Transversal to the line

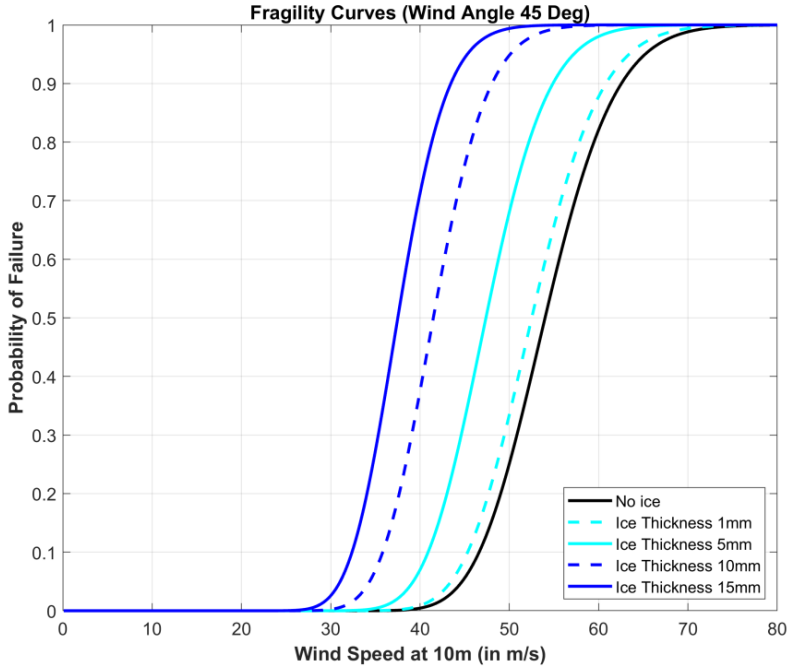

Figure 5.2: Fragility curves for Initial Dead-End Tower and Wind Angle of 45 Degrees

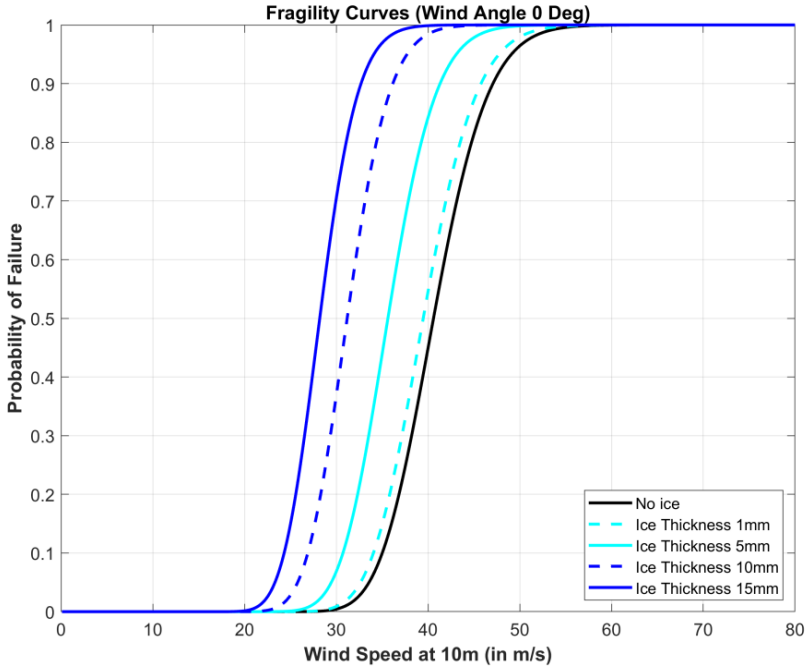

Figure 5.3: Fragility curves for Initial Dead-End Tower and Wind longitudinal to the line

5.2.2 Risk Estimation

The risk of the initial dead-end tower was estimated by combining the results of fragility (Section 5.2.1) and the corresponding site hazard (Section 4.1) following the methodology described in Section 2.3.

Table 5.2 shows the results of the risk estimation for the initial tower for the selected site of installation.

Table 5.2: Risk Estimation Results for the Initial Dead-End Transmission Tower

Risk	Annaberg -Buchholz
λ (yr^{-1})	5.90E-07
Return Period (yrs)	1.70E+06
Probability of Failure in 60yrs	3.54E-05

The results show that the annualized probability of failure is very low and much lower than the suspension tower. In specific the estimated probability of failure during the tower's service life (which is assumed to be 60 years) is 3.54E-05. The above findings are reasonable and should be attributed to the larger strength of the Dead-End tower.

5.3 Risk of Corroded Tower

The second version of the Dead-End transmission tower was a corroded version of the initial tower. The assumptions for estimation of the corrosion effect and the resulting loss in structure members were presented in Section 4.4 of [10].

5.3.1 Tower's Fragility

Table 5.3 shows the parameters of the fragility curves for the fifteen scenarios considered as in the case of the initial tower following the same assumptions in terms of the tower orientation. The corresponding fragility curves are depicted in Figure 5.4 through Figure 5.6. In terms of the effect of ice thickness and the wind angle on the parameters, the findings are similar to those of the case of the initial tower (Table 5.1). However, it should be noted that similarly to the case of the corroded telecommunication tower, all the median wind speeds are remarkably lower. This means that the corroded version of the tower is expected to fail in lower wind speeds than the initial tower. This finding should be attributed to the lower strength of the corroded tower members due to the loss of steel (reduced cross-section thickness). Moreover, the effect of wind angle is similar to that of the initial design showing that the Dead-End tower is more vulnerable for winds in the longitudinal direction.

Table 5.3: Fragility Parameters for the Corroded Dead-End Tower

Ice Thickness (mm)	Wind Angle 90°		Wind Angle 45°		Wind Angle 0°	
	Median (m/s)	Dispersion	Median (m/s)	Dispersion	Median (m/s)	Dispersion
0	58.56	0.0263	51.50	0.0279	39.16	0.0323
1	57.73	0.0289	50.76	0.0249	38.60	0.0303
5	52.95	0.0129	46.56	0.0239	35.41	0.0333
10	46.06	0.0029	40.50	0.0269	30.80	0.0333
15	40.78	0.0003	35.86	0.0249	27.27	0.0303
Mean Dispersion		0.0143		0.0257		0.0319
Total Dispersion		0.1109		0.1130		0.1145

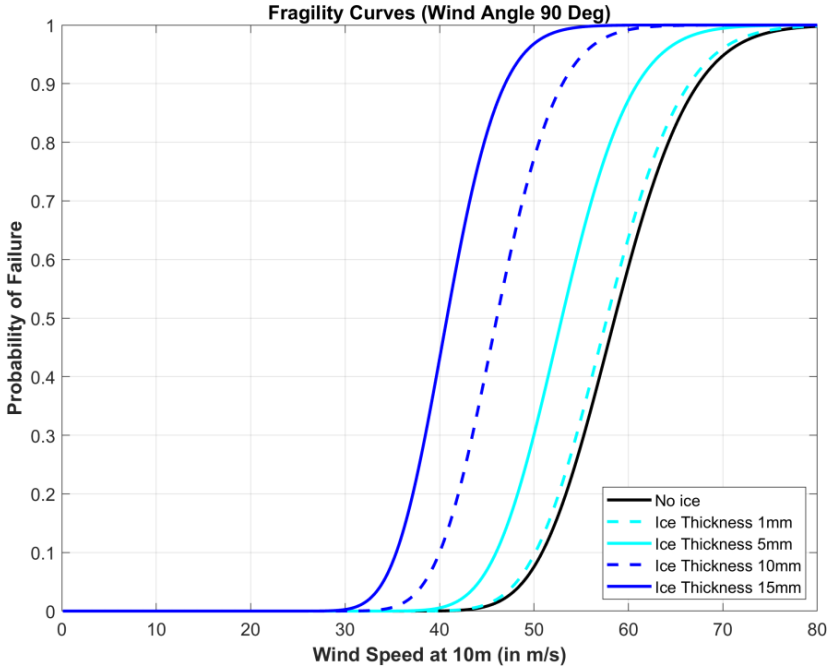

Figure 5.4: Fragility curves for Corroded Dead-End Tower and Wind Angle Transversal to the line

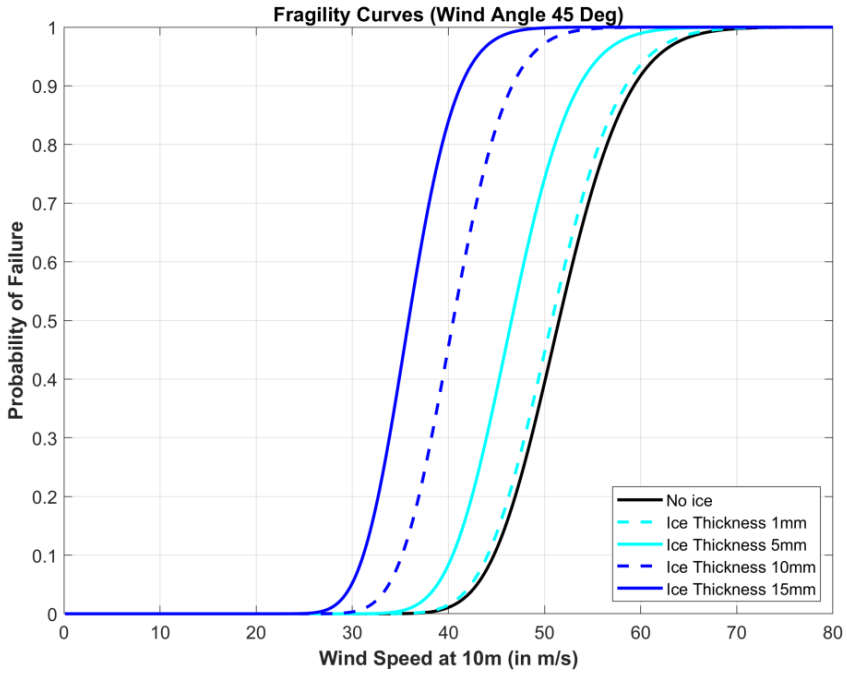

Figure 5.5: Fragility curves for Corroded Dead-End Tower and Wind Angle of 45 Degrees

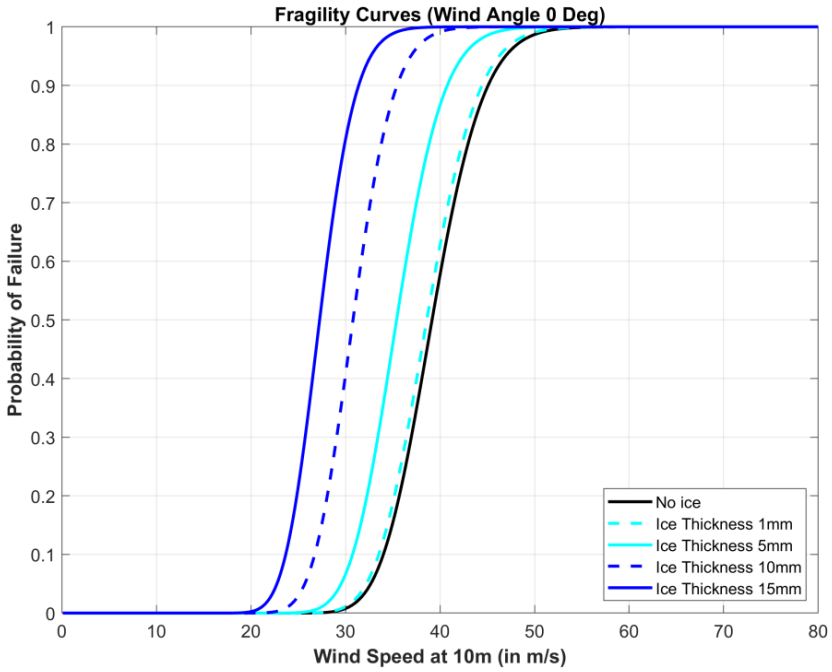

Figure 5.6: Fragility curves for Corroded Dead-End Tower and Wind longitudinal to the line

5.3.2 Risk Estimation

The risk of the corroded tower was estimated following the same process as in the case of the initial tower. The corresponding results are shown in Table 5.4.

Table 5.4: Risk Estimation Results for the Corroded Dead-End Transmission Tower

Risk	Annaberg -Buchholz
λ (yr^{-1})	8.70E-07
Return Period (yrs)	1.15E+06
Probability of Failure in 60yrs	5.22E-05

As expected, the corresponding probability of failure is higher (and the return period lower) than in the case of the initial tower. This finding should be attributed to the higher fragility of the corroded tower in comparison to the initial one. Nevertheless, even a corroded version of the Dead-End tower seems to have an extremely low probability of failure (equal to 5.22E-05) during the 60 years of its service life.

5.4 Risk of Strengthened Hybrid Member Tower

The third version of the Dead-End transmission tower was a strengthened version of the corroded tower with hybrid members strengthened via FRP plates. The methodology of strengthening was presented in Section 4.5 of [10].

5.4.1 Tower's Fragility

Table 5.5 shows the parameters of the fragility curves for the fifteen scenarios of ice thickness and wind angle combinations. The corresponding fragility curves are depicted in Figure 5.7 through Figure 5.9. In terms of the effect of ice thickness and the wind angle on the parameters, the findings

are similar to those of the cases of the initial and corroded towers. All the median wind speeds fall between their corresponding values of the initial (Table 5.1) and the corroded tower (Table 5.3). This means that the examined scenario of strengthening via FRP plates certainly increases the strength of the corroded tower but it is not sufficient to reach the strength of the initial tower. A similar result was revealed and in the case of the telecommunication tower (Section 3.4).

Table 5.5: Fragility Parameters for the Strengthened Hybrid Member Dead-End Tower

Ice Thickness (mm)	Wind Angle 90°		Wind Angle 45°		Wind Angle 0°	
	Median (m/s)	Dispersion	Median (m/s)	Dispersion	Median (m/s)	Dispersion
0	60.34	0.0159	53.56	0.0158	40.27	0.0333
1	58.46	0.0185	51.88	0.0168	39.01	0.0363
5	53.45	0.0179	46.60	0.0188	35.67	0.0343
10	47.00	0.0028	40.98	0.0158	31.36	0.0353
15	41.89	0.0167	36.52	0.0178	27.95	0.0363
Mean Dispersion		0.0144		0.0170		0.0351
Total Dispersion		0.1109		0.1113		0.1155

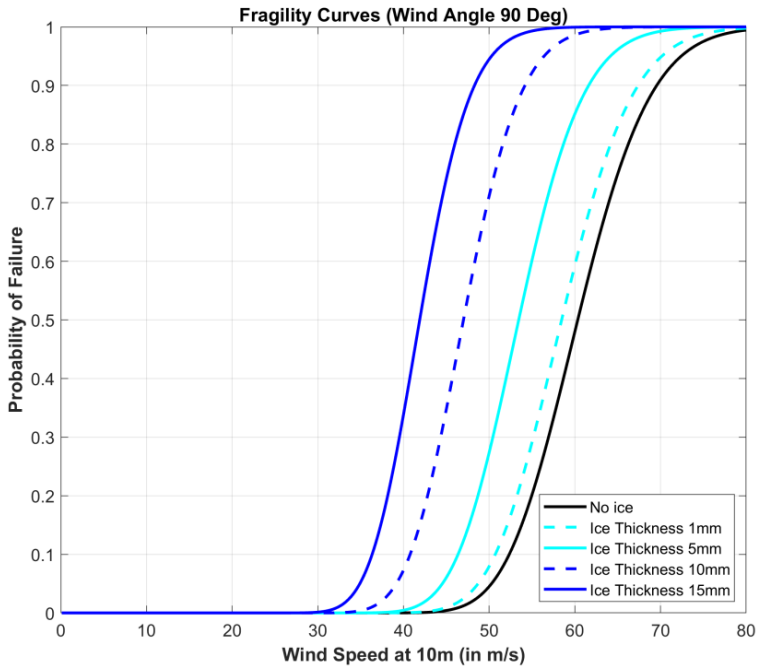

Figure 5.7: Fragility curves for Strengthened Hybrid Member Dead-End Tower and Wind Angle Transversal to the line

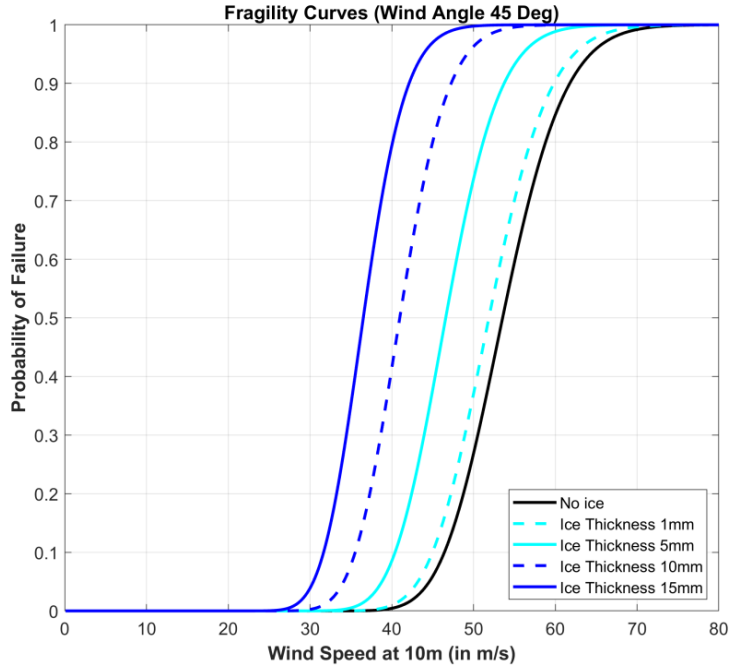

Figure 5.8: Fragility curves for Strengthened Hybrid Member Dead-End Tower and Wind Angle of 45 Degrees

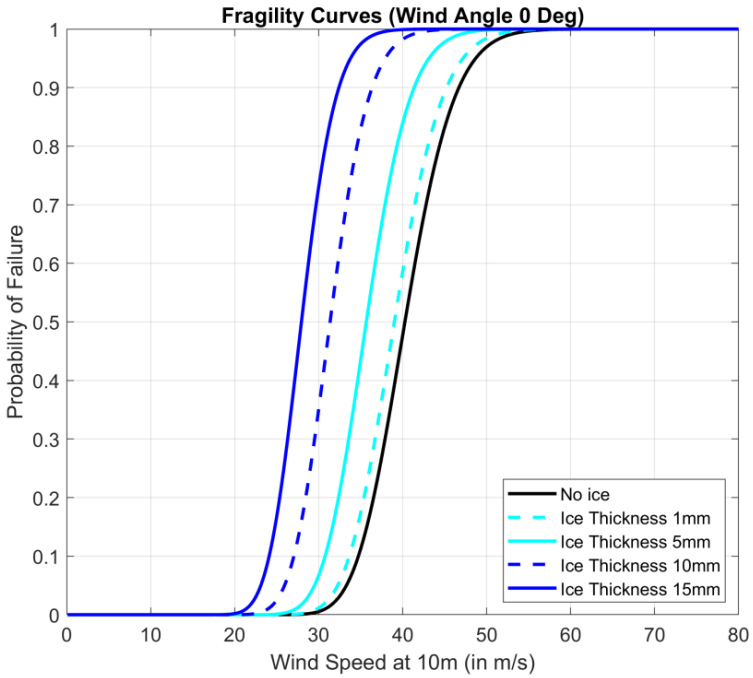

Figure 5.9: Fragility curves for Strengthened Hybrid Member Dead-End Tower and Wind longitudinal to the line

5.4.2 Risk Estimation

The results of the risk estimation for this version of tower are shown in Table 5.6.

Table 5.6: Risk Estimation Results for the Strengthened Hybrid Member Dead-End Transmission Tower

Risk	Annaberg -Buchholz
λ (yr^{-1})	6.40E-07
Return Period (yrs)	1.56E+06
Probability of Failure in 60yrs	3.84E-05

As expected, the results of the risk estimation when compared with those of the initial (Table 5.2) and corroded towers (Table 5.4) follow the same trend with the results of fragility. In other words, all values fall between their corresponding values of corroded and initial versions.

5.5 Risk of High Strength Steel Tower

The fourth version of the Dead-End transmission tower was a redesigned tower, having the same geometry with the initial tower, but with High Strength Steel (HSS) members. The specifications of the HSS version of the tower were presented in Section 4.6 of [10].

5.5.1 Tower's Fragility

Table 5.7 shows the parameters of the fragility curves for the fifteen scenarios of ice thickness and wind angle combinations. The corresponding fragility curves are depicted in Figure 5.10 through Figure 5.12. In the case of HSS tower, the corresponding median wind speeds of failure are close to the case of the initial model (Table 5.1). A similar finding was observed in the case of the suspension transmission tower (Section 4.4). Finally, it is noteworthy that this similar strength was achieved in spite of the fact that the HSS Dead-End tower weighs less than the tower designed with conventional steel by around 4.0 tons.

Table 5.7: Fragility Parameters for the HSS Dead-End Tower

Ice Thickness (mm)	Wind Angle 90°		Wind Angle 45°		Wind Angle 0°	
	Median (m/s)	Dispersion	Median (m/s)	Dispersion	Median (m/s)	Dispersion
0	60.10	0.0242	53.34	0.0150	40.10	0.0313
1	58.21	0.0282	51.46	0.0140	38.69	0.0353
5	53.18	0.0259	47.01	0.0110	35.34	0.0333
10	46.51	0.0000	41.11	0.0100	30.91	0.0353
15	41.20	0.0247	36.42	0.0080	27.38	0.0333
Mean Dispersion		0.0206		0.0116		0.0337
Total Dispersion		0.1119		0.1106		0.1150

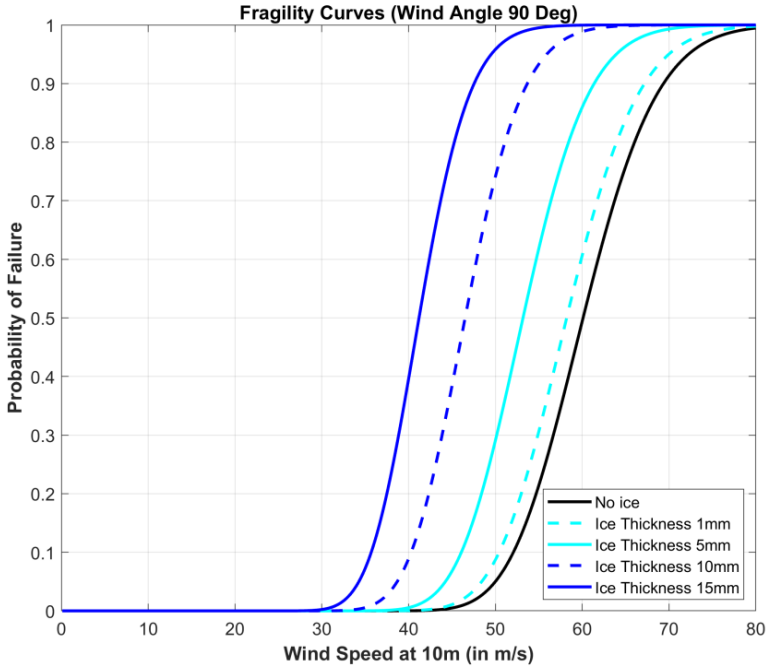

Figure 5.10: Fragility curves for HSS Dead-End Tower and Wind Angle Transversal to the line

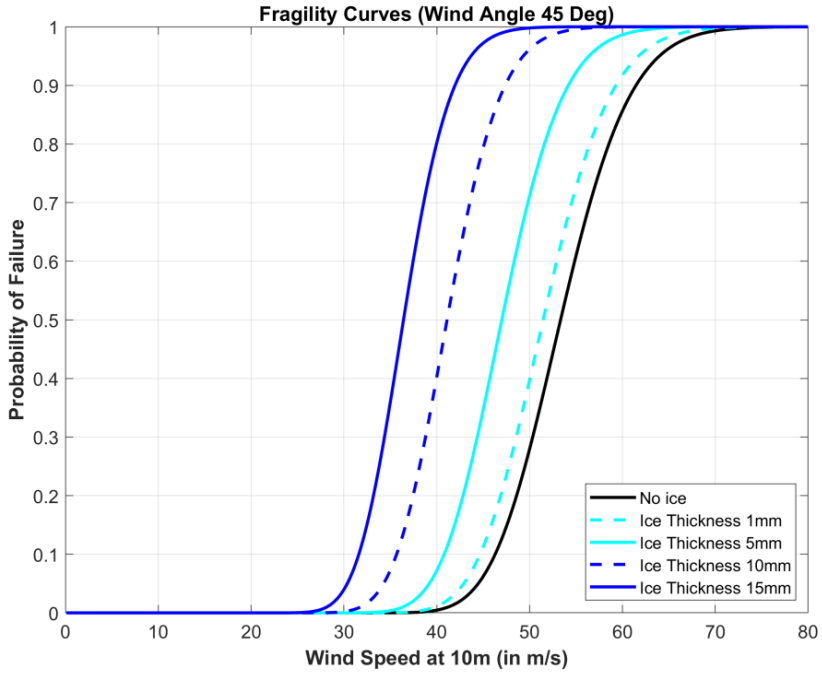

Figure 5.11: Fragility curves for HSS Dead-End Tower and Wind Angle of 45 Degrees

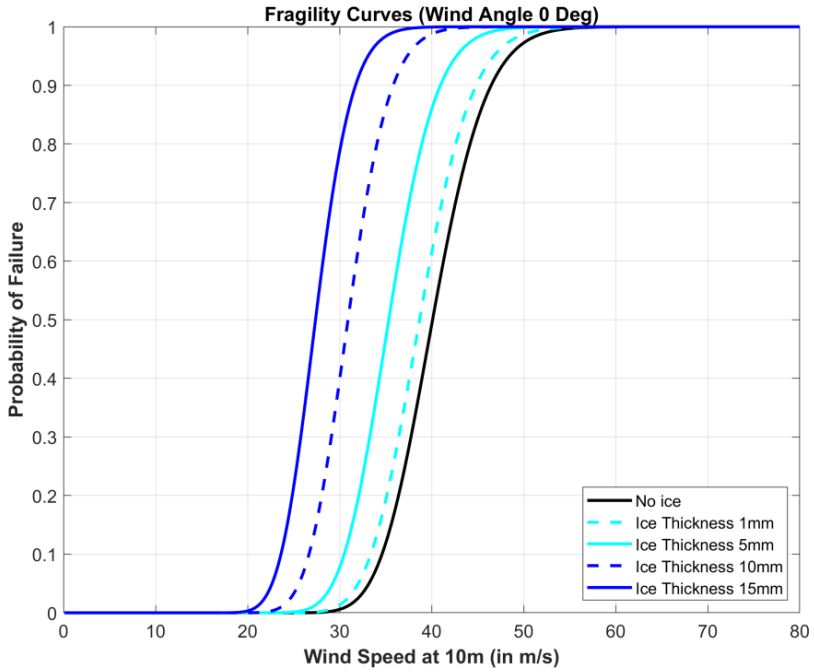

Figure 5.12: Fragility curves for HSS Dead-End Tower and Wind longitudinal to the line

5.5.2 Risk Estimation

The results of the risk estimation for the HSS suspension transmission tower are shown in Table 5.8.

Table 5.8: Risk Estimation Results for the HSS Dead-End Transmission Tower

Risk	Annaberg -Buchholz
λ (yr^{-1})	7.97E-07
Return Period (yrs)	1.25E+06
Probability of Failure in 60yrs	4.78E-05

As expected, the probability of failure is much lower in comparison with the corroded tower. However, is larger to those of the initial design and the strengthened hybrid member Dead-End tower. This is an interesting effect of the trade-off between the structure's weight and its strength.

6 Case Study 4: Transmission Line in Germany

In Sections 4 and 5 of the present, the risk estimation of two types (Suspension and Dead-End) of an individual power transmission tower was presented for a specific site in Central-East Germany and four various versions of the status of the tower (e.g. initial design, corroded state etc.)

In this Section the results of Sections 4 and 5 will be used in order to perform an estimation of the risk of power line segment that is consisted of the aforementioned transmission towers. In other words, the information regarding the fragility of the individual towers, the hazard of their location and the associated risk will be combined in order to estimate the risk of a power transmission line segment.

6.1 Description

A power line (segment) with six spans (with a length of 350m each) with three Dead-End towers (shown in red) and four suspension towers (shown in green) was considered (Figure 6.1). Furthermore, it was assumed that the full power line does not deviate from the straight line.

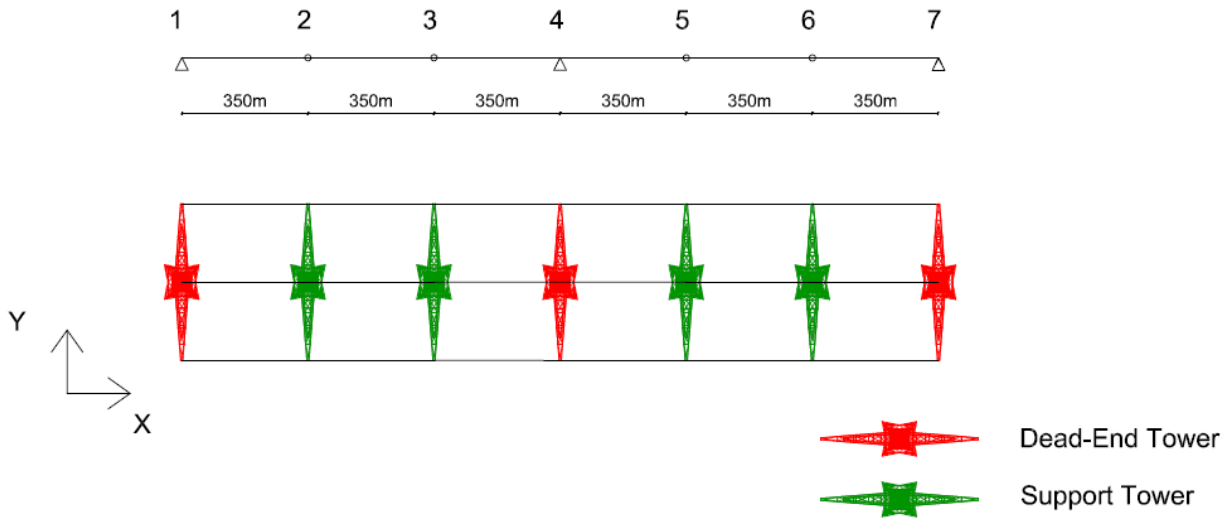

Figure 6.1: Full Power Line Model

6.2 Methodology

The estimation of the line's fragility was performed via Monte Carlo simulation based on the fragilities of the two individual towers. In specific, for each scenario of wind speed, wind angle and ice thickness combination and each tower (suspension and dead-end), 1000 realizations were generated. Those realizations consist of values 0 and 1, where value 1 represents the failure of the tower. The percentages of 1(tower failure) are related to the probability that the specific tower (suspension or Dead-End) will fail for that hazard scenario (Sections 4.2-4.4 and 5.2-5.5).

The full power line fails even if one of the towers fails. The probability of line failure for each scenario is estimated by simply dividing the number of failures by the total number of realizations.

At the end of the process, the risk of the transmission line for the site of Annaberg-Buchholz shown in Figure 4.1 can be estimated by combining the results of fragility, produced from Monte Carlo simulation, and the estimated hazard for the site of Marienberg (Section 4.1) following the methodology shown in Section 2.3. The total annualized probability of failure λ is calculated by applying Eq. (2.5). Finally, the corresponding Return Period can be calculated by Eq. (2.6), while the probability of failure during the service life of tower (e.g. 60 years) by Eq. (2.7)

6.3 Risk of Line with Conventional Designed Towers

The first scenario of the power line examined herein considered that both the suspension and the Dead-End tower were at their initial design with conventional steel. So, the fragility and the risk results presented in Sections 4.2 and 5.2 were used.

Table 6.1 shows the results of the risk estimation for the transmission line with conventional designed towers.

Table 6.1: Risk Estimation Results for the Line with Initial Towers

Risk	Line
λ (yr^{-1})	4.13E-04
Return Period (yrs)	2422.58
Probability of Failure in 60yrs	0.025

According to Table 6.1 the probability of failure of the whole power line segment is 2.5% during its service life.

6.4 Risk of Line with Corroded Towers

The second scenario of the power line considered that both the suspension and the Dead-End towers were at the corroded state examined at Sections 4.3 and 5.3.

Table 6.2 shows the results of the risk estimation for the transmission line with corroded towers.

Table 6.2: Risk Estimation Results for the Line with Corroded Towers

Risk	Line
λ (yr^{-1})	1.62E-03
Return Period (yrs)	616.78
Probability of Failure in 60yrs	0.093

According to Table 6.2 the probability of failure of the whole power line segment is 9.3% during its service life. The above value (as expected) is higher than that of the case of the initial towers.

6.5 Risk of Line with Strengthened Hybrid Member Towers

The third scenario of the power line considered that the suspension tower was at the corrode state (Section 4.3) while the Dead-End tower was strengthened via FRP plates (Section 5.4).

Table 6.3 shows the results of the risk estimation for the transmission line of the above scenario.

Table 6.3: Risk Estimation Results for the Line with Strengthened Hybrid Member Dead-End Towers

Risk	Line
λ (yr^{-1})	1.62E-03
Return Period (yrs)	616.02
Probability of Failure in 60yrs	0.093

According to Table 6.3 the probability of failure of the whole power line segment is exactly the same as the case when both types of towers were assumed to be at the corroded state.

6.6 Risk of Line with High Strength Steel Towers

The fourth scenario of the power line considered that both the suspension tower and the Dead-End tower were made by HSS (Sections 4.4 and 5.5).

Table 6.4 shows the results of the risk estimation for the transmission line with High Strength Steel towers.

Table 6.4: Risk Estimation Results for the Line with High Strength Steel Towers

Risk	Line
λ (yr^{-1})	5.93E-04
Return Period (yrs)	1678.04
Probability of Failure in 60yrs	0.035

It comes out that the probability of failure of the whole power line segment is lower than the case of the corroded towers but higher than the case of the towers of the initial design. This is in accordance with the results of risk estimation for the individual towers.

6.7 Conclusions

Based on the results of the previous sections it is concluded that the line with conventional designed towers has the lowest probability of failure (2.5% during its service life). The line with HSS towers follows with 3.5% and finally both lines with corroded and strengthened hybrid member (Dead-End) towers have the larger probability of failure equal to 9.3%.

It is noteworthy that the power transmission line under study was considered as a serial system with non-correlated towers. Thus, the weakest parts control the risk of the line. In this case suspension towers are the weakest components of the line compared with Dead-End towers. This assumption results to a line risk higher than the risk of the weakest tower. Finally, this is the reason why transmission lines, even with strengthened hybrid member Dead-End towers but having corroded suspension towers, are subject to exactly the same risk with lines where all their towers (suspension and Dead-End) are corroded.

7 Cost-Benefit Analyses

7.1 Baseline rehabilitation options

After exhausting a service life of 60yrs, the three towers assessed in Sections 3-5, namely the antenna, support and dead-end towers, and the entire powerline of Section 6 stand corroded. The owner needs to take action and is faced with the following options:

a. Do Nothing: This is the typical option due to lack of funds, or when the risk of failure is considered to be low despite the corrosion damage.
b. Replace Conventional: This is a full replacement of the tower with an identical one, made of the same members and structural steel. Only the foundation is maintained due to the similar dimensions and little to no corrosion damage.[1]
c. Replace HSS: This is a full replacement of the tower with a new one made of high-strength steel angles, as per D4.1 [10]. Due to having the same dimensions, the foundation is maintained.
d. Strengthen FRP: This is a partial strengthening scheme, where FRP plates are locally applied to critical corroded members, as per D4.1 [10].

In the case of the power-line, for options b-d, only the support towers are replaced or strengthened.

Note that a conventional strengthening scheme, whereby critical corroded members would simply be replaced by equivalent non-corroded ones, is not considered. While this is a competitive option when only brace members are involved, it is not as applicable when legs need to be replaced. Other strengthening options that would not involve removal of sections, such as adding angles to critical members to form a stronger battened section, are also not considered.

To price options, the following basic assumptions are also made for all four:

i. Corrosion progression is inhibited in all cases, employing, e.g., cathodic protection measures for a & d and improved zinc coating for c & d, which are assumed to be of the same cost in all cases. This cost is thus not accounted for, making the cost of the Do Nothing approach exactly zero.
ii. The total length of members upgraded by FRP is considered to be the same for both the support and the dead-end tower (for which it has been actually estimated) due to following the same strengthening pattern for the same overall length of steel members. The strengthened support tower is assumed to achieve a collapse return period equal to the average of the initial and the HSS tower, similar to what happens for the dead-end tower. The cost of the FRP is applied in addition to the cost of conventional strengthening of the towers, to include transportation, labor, preparation of surfaces, protective painting etc.
iii. HSS costs ~40€/ton of steel, or roughly 2% more given a market price of 2,000 €/ton of S355 steel. About ¾ of the HSS tower is made of HSS steel, meaning a surcharge of 1.5% over the conventional steel tower on a ton-by-ton basis.
iv. For the powerline, only the four support towers are replaced or upgraded. The Do Nothing option is employed by default for the dead-end ones.
v. The antenna requires coloring and lighting. Transmission towers do not, as it is assumed they are not close to an airport.
vi. The overall depreciation rate is assumed to remain constant at the current ~0.0% for the next 60 years.
vii. Any potential consistent changes from current weather patterns are disregarded.

[1] There have been cases where the foundation reinforcement was found to have worse corrosion than the exposed tower, but this is typically the unusual case of having unacceptable aggregates in the foundation concrete (e.g., beach sand).

Table 7.1: Initial construction costs for 48m antenna tower for Greece

Task	**Cost (€)**
Procurement (manufacturing, bolts etc.)	47552.82
Transport and Installation	15075.77
Tower foundation (excavations, grounding etc.)	19289.10
Coloring	6669.63
Lighting	4900.52
Total	93487.84

Table 7.2: Materials needed for implementing rehabilitation option strategy

	Steel weight (ton) or S512 FRP length (m)			
Strategy	Antenna	Support	Dead-end	Line
Do Nothing	0	0	0	0
Replace Conventional	15.14t	16.99t	66.32t	67.96t
Replace HSS	14.03t	15.99t	56.24t	63.96t
Strengthen FRP	156m	97m	194m	388m

Table 7.3: Initial costs for implementing each rehabilitation option strategy

	Upfront initial costs (€)			
Strategy	Antenna	Support	Dead-end	Line
Do Nothing	0	0	0	0
Replace Conventional	74,199	68,439	223,378	273,757
Replace HSS	71,373	66,052	194,368	264,207
Strengthen FRP	25,663	23,521	27,042	94,084

Table 7.4: Collapse return periods

	Collapse return period (yrs)			
Strategy	Antenna	Support	Dead-end	Line
Do Nothing	504	1357	1.15E+06	617
Replace Conventional	1589	5436	1.70E+06	2423
Replace HSS	5797	3537	1.25E+06	1678
Strengthen FRP	1045	4486	1.56E+06	2019

For the antenna, direct costs for a single tower are provided from the market as per Table 7.1. In addition, the cost to the telecommunication company for performing conventional strengthening on an existing tower of the given size (48m high) is estimated at 20,000€. The costs of all other towers are extrapolated from the above values on a weight basis (see Table 7.2), applying any surcharge due to HSS, neglecting coloring and lighting for powerline towers, and disregarding foundation costs for all cases, as stated earlier. For FRP, strengthening by the application of S512 FRP plates is assumed for the antenna and the support tower. For the dead end, the same length of plates as with the support tower is employed, only now S1012 FRP plates are used instead, having twice the cost, thus double the length is reported in Table 7.2. The cost of an S512 plate is 30€/m, with an additional 6.3€/m for the adhesive product. The overall initial costs per each strategy appear in Table 7.3.

Table 7.4 summarizes the return periods of collapse per each scenario, according to the findings of Sections 3-6. To assess the average annual loss (AAL) due to collapse events, based on a Poisson occurrence process for storm events and given the 0% interest, one need only divide the event losses by the corresponding return period. Table 7.5 contains the direct AAL, assuming each collapsed tower is replaced by a new conventional one, per typical practice.

Table 7.5: Direct Average Annual Loss

	Direct Average Annual Loss (€)			
Strategy	Antenna	Support	Dead-end	Line
Do Nothing	147	50	0	444
Replace Conventional	47	13	0	113
Replace HSS	13	19	0	163
Strengthen FRP	71	15	0	136

7.2 Case study scenarios

For the telecommunication antenna in Greece, only the intermediate weather scenario of Samothraki is considered, as both Finokalia and Zagora are on opposite extremes, the first being too aggressive and the latter too benign. Given that indirect losses due to service disruption (i.e., loss of revenue) are likely to supersede the direct losses of tower replacement, the size of the population served by the tower matters. Thus, one low and one high scenario are considered. First is the island of Samothraki, with a population of 3,055 permanent residents, assumed to double over the three summer months for a yearly average of 3,819. A single tower is assumed to serve the telecommunication needs of the entire island. The second location is the nearby coastal town of Kavala, with similar weather characteristics and a population of 70,501 residents. The average revenue per resident is assumed to be 30€/month, and a disruption event is assumed to take 10 days to resolve, during which the telecommunication company cannot charge consumers. Additional contractual penalties are not considered. Thus, the cost of one disruptive event is 34,369€ for Samothraki, and 634,509€ for Kavala.

The power transmission line in Germany is considered as a regional branch that could serve two potential areas. First are the towns of Annaberg-Buchholz and Marienberg having 19,619 and 16,906 residents, respectively with a combined total of 36,525. Second is the overall district of Erzgebirgskreis, which contains the two towns, with 334,948 residents. The average revenue for the power company is 125€/month per person (incorporating both transmission and generation costs) and the disruption event is assumed to result to a 10-day blackout, or loss of one third of the monthly

revenue, disregarding potential contractual penalties. Thus, the cost of one disruptive event is 1,369,688€ for Annaberg-Buchholz & Marienberg, and 12,560,550€ for Erzgebirgskreis.

Table 7.6: Indirect Average Annual Loss (small-scale scenarios)

	Indirect Average Annual Loss (€)			
Location	Samothraki	Annaberg-Buchholz & Marienberg		
Strategy	Antenna	Support	Dead-end	Line
Do Nothing	68	1009	1	2221
Replace Conventional	22	252	1	565
Replace HSS	6	387	1	816
Strengthen FRP	33	305	1	678

Table 7.7: Indirect Average Annual Loss (large-scale scenarios)

	Indirect Average Annual Loss (€)			
Location	Kavala	Erzgebirgskreis		
Strategy	Antenna	Support	Dead-end	Line
Do Nothing	1259	9256	10.92	20365
Replace Conventional	399	2311	7.39	5185
Replace HSS	109	3551	10.05	7485
Strengthen FRP	607	2800	8.05	6222

7.3 Lifecycle cost estimates

As per the direct AAL estimates, the indirect costs of AAL due to the revenue loss caused by service disruption can be estimated by dividing the per event costs by the collapse return periods. Tables 7.6 and 7.7 show the results for the small-scale (Samothraki, Annaberg-Buchholz & Marienberg) and versus large-scale scenarios (Kavala, Erzgebirgskreis). By extending to a projected service life of 60yrs and adding the upfront initial costs, the total aggregated cost per each rehabilitation strategy can be estimated, as shown in Tables 7.8 and 7.9.

What is abundantly clear, is that the Do Nothing approach is the most competitive for the dead-end tower, thanks to its sturdy construction. Still, the case of asymmetric loading, where support towers on one side have collapsed has not been considered. This is clearly the critical case that governs collapse for longer powerlines. It may not be as critical for the shorter 7-tower line considered, yet that conclusion may change for longer branches and main backbones of the power transmission network. Otherwise, from a pure monetary standpoint, the optimal strategy depends on the population served. If the population is large enough, selective strengthening is the best option for both telecommunication and power transmission applications. For smaller service areas such as Samothraki, it is not worth spending money on extended repairs. Then, a Do Nothing approach can be quite competitive, assuming some measures are taken to inhibit the progression of corrosion. Replacement does not seem to be as competitive, given that the cheaper strengthening can achieve similar return periods at a much-reduced cost. Still, an initial construction based on the HSS tower is undeniably superior to any conventional steel tower in terms of upfront cost. When aggregated over

the service lifetime, the benefits depend on the case study at hand, as the higher optimization in the design of the HSS tower also comes with a lower overstrength and an associated lower collapse return period. An HSS replacement strategy can also become viable in cases of more aggressive corrosion than the one considered herein, something to be kept in mind for future studies.

Table 7.8: Total aggregated loss over 60yrs (small-scale scenarios). Optimal strategies are indicated in bold

	Total 60yrs Loss (€)			
Location	Samothraki	Annaberg-Buchholz & Marienberg		
Strategy	Antenna	Support	Dead-end	Line
Do Nothing	**12,921**	63,583	**83**	159,873
Replace Conventional	78,299	84,313	223,435	314,460
Replace HSS	72,497	90,449	194,445	322,970
Strengthen FRP	31,896	**42,754**	27,103	**142,927**

Table 7.9: Total aggregated loss over 60yrs (large-scale scenarios). Optimal strategies are indicated in bold

	Total 60yrs Loss (€)			
Location	Kavala	Erzgebirgskreis		
Strategy	Antenna	Support	Dead-end	Line
Do Nothing	84,348	558,360	**667**	1,248,514
Replace Conventional	100,962	207,833	223,830	591,624
Replace HSS	78,709	280,296	194,982	723,110
Strengthen FRP	**66,352**	**192,419**	27,534	**475,514**

References

[1] Baker, J.W., Efficient analytical fragility function fitting using dynamic structural analysis. Earthquake Spectra (31), 579-599, 2015.

[2] Paschen, R., Pezard, J., Zago, P., Probabilistic evaluation on test results of transmission line towers. International Conference on Large High Voltage Electric Systems, 28th Aug.- 3rd Sep. 1988, Paris, France.

[3] Makkonen, L., Estimation of wet snow accretion on structures. Cold Regions Science and Technology (17), 83-88, 1989.

[4] Makkonen, L., Ahti, K., Climatic mapping of ice loads based on airport weather observations. Atmospheric Research (36), 185-193, 1995.

[5] Sundin, E., Makkonen, L., Ice Loads on a Lattice Tower Estimated by Weather Station Data. Journal of Applied Meteorology (37), 523-529, 1998.

[6] Makkonen, L., Lehtonen, P., Hirviniemi, M., Determining ice loads for tower structure design. Engineering Structures (74), 229-232, 2014.

[7] Jones, K., Ice accretion in freezing rain. CCREL Report96-2, U.S. Army Corps of Engineers, 1996.

[8] Jones, K., A simple model for freezing rain ice loads. Cold Atmospheric Research (46), 97-97, 1998.

[9] Lee, C.; Wang, Y.-J., A novel method to derive formulas for computing the wet-bulb temperature from relative humidity and air temperature. Measurement (128), 271-275, 2018.

[10] ANGELHY Deliverable 4.1, Parametric Models of Case Studies and Loads, Research Program of the Research Fund for Coal and Steel ANGELHY, Grant Agreement Number: 753993, European Commission, Brussels, Belgium, 2020.

List of Figures

List of Tables

ANNEX – Additional information

The results of the fragility estimation for each structure could be associated with the basic design wind speed of the structure. To do so, the values of wind speed U_{10} of the x-axis of the fragility curves could be simply divided by the value of the basic wind speed (V_b). Herein, the basic wind speed for the telecommunication towers is $V_b = 33\ \mathrm{m/s}$, while for the power transmission towers is $V_b = 25\ \mathrm{m/s}$.

Figure A-1 through Figure A-3 present the corresponding fragility curves for the three types of lattice towers considered in this task at their initial, corroded and HSS versions. It is noteworthy that only the curves of the scenario of no ice conditions and wind angle of attack of 90° are presented for the sake of brevity.

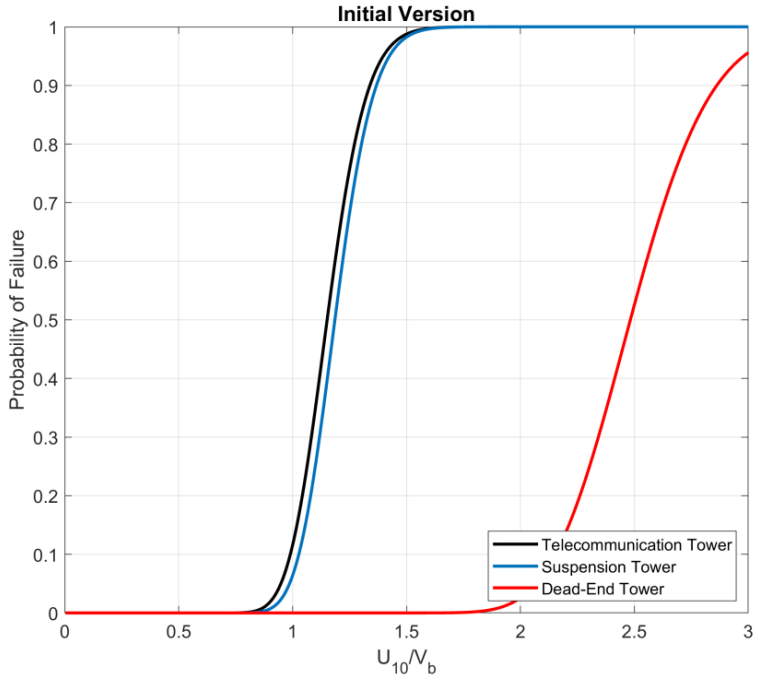

Figure A-1: Fragility Curves for the Initial Versions of the Three Lattice Towers

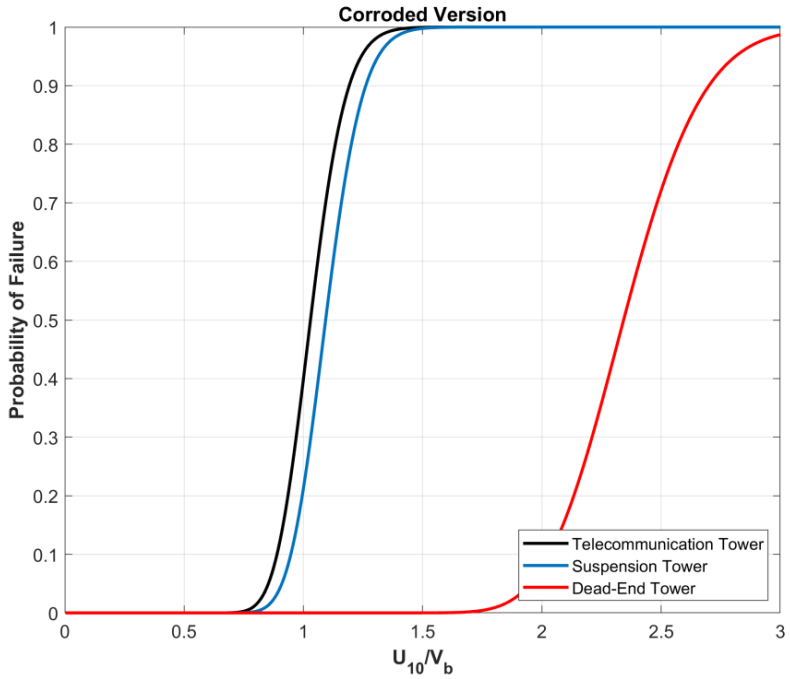

Figure A-2: Fragility Curves for the Corroded Versions of the Three Lattice Towers

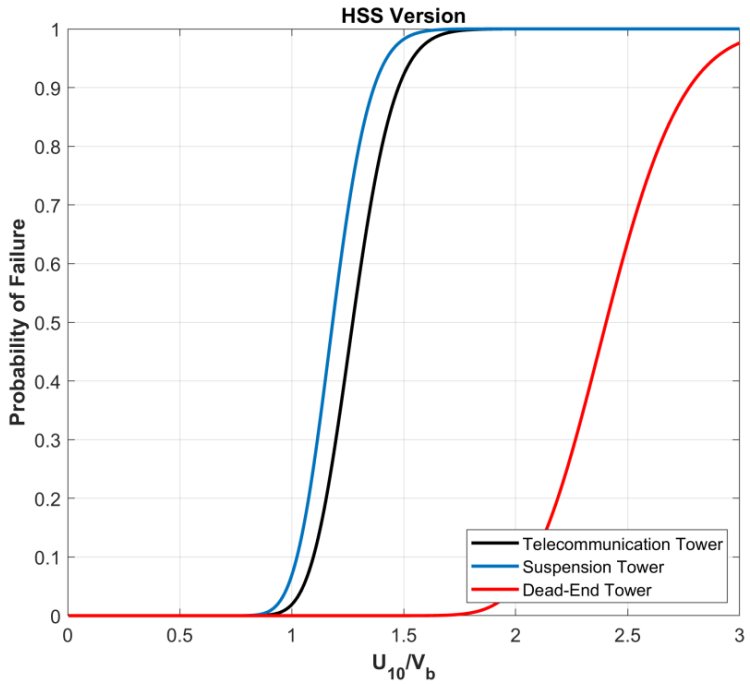

Figure A-3: Fragility Curves for the HSS Versions of the Three Lattice Towers

From the above graphs it is observed that in all cases the strength of the Dead-End transmission tower is remarkably large, especially if it is compared with the telecommunication and the suspension transmission towers. In specific, the median wind speed of failure for the initial and the HSS versions of the Dead-End transmission tower is about 2.5 times larger than the basic design wind speed. In the case of the corroded version, the median wind speed is quite lower (as expected) but again is close to 2.3 times larger than the basic wind speed.

Regarding the telecommunication and the suspension transmission towers, the corresponding fragility curves show similar trends. The median wind speed for the initial and HSS version of both towers is around 1.25 times larger than the basic wind speed. For the corroded versions the median wind speed drops and it is close to 1.02 times larger than the basic wind speed for the telecommunication tower and 1.10 times for the suspension tower.

Finally, all versions of the telecommunication and the suspension transmission towers have a probability of failure equal to 1 when the wind speed is two times the basic wind speed. For the Dead-End transmission tower though this value should be larger than 3 times the basic wind speed in all versions of the tower.